Wolters Kluwer Health | Lippincott Williams & Wilkins

EUROPEAN SOCIETY OF CARDIOLOGY®

Original Scientific Paper

Effect of lipid-lowering therapy with atorvastatin on atherosclerotic aortic plaques: a 2-year follow-up by noninvasive MRI

Atsushi Yonemura[a], Yukihiko Momiyama[c], Zahi A. Fayad[d], Makoto Ayaori[a], Reiko Ohmori[a], Teruyoshi Kihara[b], Nobukiyo Tanaka[a], Kazuhiro Nakaya[a], Masatsune Ogura[a], Hiroaki Taniguchi[a], Masatoshi Kusuhara[a], Masayoshi Nagata[b], Haruo Nakamura[a], Seiichi Tamai[a] and Fumitaka Ohsuzu[a]

[a]National Defense Medical College, [b]Iruma Heart Hospital, Saitama, [c]National Hospital Organization Tokyo Medical Center, Tokyo, Japan and [d]Mount Sinai School of Medicine, New York, USA

Received 12 July 2008 Accepted 12 January 2009

Background Using MRI, we reported plaque regression in thoracic aorta and retardation of plaque progression in abdominal aorta by 1-year atorvastatin. However, association between serial plaque changes and LDL-cholesterol levels was not fully elucidated.

Design A prospective, randomized, open-label trial.

Methods We investigated the long-term effect of 20 versus 5-mg atorvastatin on thoracic and abdominal plaques and the association between plaque progression and on-treatment LDL-cholesterol levels in 36 hypercholesterolemic patients. MRI was performed at baseline and 1 and 2 years of treatment. Vessel wall area change was evaluated.

Results The 20-mg dose markedly reduced LDL-cholesterol levels (−47%) versus 5-mg (−35%) dose. After 2 years of treatment, regression of thoracic plaques was found in the 20-mg group (−15% vessel wall area reduction), but not in the 5-mg group (+7%). Although the 20-mg dose induced plaque regression (−14%) from baseline to 1 year, no further regression was seen from 1 to 2 years of treatment (−1%). Regarding abdominal plaques, progression was found in the 5-mg group (+10%), but not in the 20-mg group (+2%). Plaque progression in the 5-mg group was found from baseline to 1 year (+8%), but not from 1 to 2 years (+2%). The degree of thoracic plaque regression correlated with LDL-cholesterol reduction ($r=0.61$), whereas thoracic plaque change from 1 to 2 years correlated with on-treatment LDL-cholesterol levels ($r=0.64$).

Conclusion Twenty milligrams of atorvastatin regressed thoracic plaques. However, maintaining low LDL-cholesterol levels was needed to prevent plaque progression. In abdominal aorta, only retardation of plaque progression was found after 2 years of 20-mg treatment. *Eur J Cardiovasc Prev Rehabil* 16:222–228 © 2009 The European Society of Cardiology

European Journal of Cardiovascular Prevention and Rehabilitation 2009, 16:222–228

Keywords: aorta, atherosclerotic plaque, lipid-lowering, MRI

Introduction

Recently, magnetic resonance imaging (MRI) has become a useful tool for the noninvasive evaluation of atherosclerotic plaques in the aorta and carotid arteries [1–4]. A good correlation regarding the aortic plaque extent was found between the MRI findings and histopathology in rabbit models [5]. In humans, the MRI evaluation of the thoracic aorta has been shown to closely correlate with transesophageal echocardiography findings [1]. Using MRI, we [6–9] and others [10] demonstrated the plaque regression in human aortas in response to lipid-lowering therapy. We recently reported the plaque regression in the thoracic aorta and the retardation of plaque progression in the abdominal aorta in response to 1-year intensive LDL-cholesterol (LDL-C) lowering with atorvastatin [8].

Correspondence to Dr Yukihiko Momiyama, MD, National Hospital Organization Tokyo Medical Center, 2-5-1 Higashigaoka, Meguro-ku, Tokyo 152-8902, Japan
Tel: +81 3 3411 0111; fax: +81 3 3412 9811; e-mail: ymomiyamajp@yahoo.co.jp

DOI: 10.1097/HJR.0b013e32832948a0

However, the association between serial plaque changes and the on-treatment LDL-C levels has not been fully elucidated. This study therefore extended our previous study by elucidating the long-term effect of 20-mg (the maximal approved dose in Japan) versus 5-mg atorvastatin on aortic plaques and the association between plaque progression and the on-treatment LDL-C levels during a 2-year follow-up in patients with hypercholesterolemia.

Methods

Study patients

Our study was a prospective, randomized, open-label trial to elucidate the effect of 20 versus 5-mg atorvastatin on thoracic and abdominal aortic plaques in asymptomatic patients with hypercholesterolemia [8]. Any patient with a history of atorvastatin treatment was excluded. If patients had been taking other statins, these drugs were discontinued for at least 4 weeks. If patients had a serum LDL-C level of greater than 150 mg/dl, they underwent aortic MRI and were randomized to receive either 20 or 5-mg atorvastatin daily. Our study was approved by the institutional ethics committee. Written informed consent was obtained from all patients. Repeat MRI was scheduled after 1 and 2 years of treatment. Of the 50 patients randomized, 10 withdrew of their own accord, and four had adverse events (one cerebral infarction, one liver dysfunction, one body eruption, and one general fatigue). As a result, 18 patients in the 20-mg group and 18 in the 5-mg group had MRI after 1 and 2 years of treatment. The lipid levels were measured by standard laboratory methods. The plasma high-sensitivity C-reactive protein (hsCRP) levels were measured by a BNII nephelometer (Dade Behring, Germany).

Aortic MRI

MRI was performed on a Signa 1.5 T Cvi scanner (GE Medical Systems, Mount Prospect, Illinois, USA) using a phased-array body coil. As we previously reported [8,9], transverse proton density-weighted (PDW) and T2-weighted (T2W) images of the thoracic descending and abdominal aortas were obtained using a double-inversion-recovery fast spin-echo sequence without a fat saturation pulse. Imaging parameters were repetition time=2 RR intervals, echo time=10 (PDW) and 60 ms (T2W), 20-cm field of view, 4-mm slice thickness, 8-mm interslice gap, 256 × 256 matrix, and 32 echo-train. At baseline, nine slices of the thoracic aorta and nine slices of the abdominal aorta were obtained at 12-mm intervals, each of which covered about the 10-cm portions of the thoracic aorta and of the abdominal aorta. Plaque was defined as a clearly identified luminal protrusion with focal wall thickening.

Regarding MRI after 1 and 2 years of treatment, special attention was paid to match the images to those at baseline. As we previously reported [8,9], for each plaque, three contiguous slices (no interslice gap) were obtained, and the slice most closely matching the one at baseline was selected using several anatomical landmarks (i.e. vertebrae, intercostal and lumbar arteries, pulmonary arteries and veins, and mesenteric arteries). The matching procedure was performed by two observers, blinded to the treatment assignment, and all discrepancies were resolved by consensus.

MRI analysis

As we previously reported [8,9], the maximal vessel wall thickness (VWT_{max}), total vascular area (TVA), and lumen area (LA) in the matched slices with plaque at baseline and 1 and 2 years of treatment were measured three times by manual planimetry using an NIH Image software package (Scion Co., Frederick, Maryland, USA) and averages were used for statistical analysis. The vessel wall area (VWA) was calculated as TVA minus LA. All measurements were made by Y.M., blinded to the treatment assignment and the order of images. The intraobserver variability for VWT and VWA measurements were 0.1 mm and 1.3 mm^2, respectively [8].

Plaque characterization was based on the signal intensities of the plaque on PDW and T2W images [1,11]. Lipid components were identified as hyperintense on PDW and hypointense regions on T2W images. Calcium deposits were identified as hypointense regions on both images. As in our previous studies [3,8,9], T1W images were omitted to reduce the examination time.

Statistical analysis

Any differences between two groups were evaluated by the unpaired *t*-test for continuous variables and by the χ^2 test for categorical variables. Any differences among baseline and after 1 and 2 years of treatment were evaluated by repeated-measure analysis of variance with the Bonferroni test for continuous variables. Correlations between the plaque changes and LDL-C levels or other factors were evaluated by Pearson's correlation coefficient. The independent associations between plaque changes and these factors were evaluated using a stepwise multiple linear regression analysis. A P value of less than 0.05 was considered to be statistically significant.

Results

At baseline, age, sex, risk factors, and lipid levels did not differ between the two groups (Table 1). The 20-mg dose markedly reduced LDL-C levels (−47%) in comparison with the 5-mg dose (−33%) ($P < 0.001$). Both the 20 and 5-mg doses also reduced hsCRP levels by −52 and −30%, respectively. However, after a period from 1 year to 2 years of treatment, no change was observed in the lipid or hsCRP levels in either group.

A total of 45 thoracic aortic plaques (25 in the 20-mg group and 20 in the 5-mg group) and 63 abdominal

Table 1 Demographic and laboratory data at baseline and after 1 and 2 years of treatment

	20-mg dose ($n=18$)							5-mg dose ($n=18$)							
	Baseline	Baseline versus 1 year	1 year	1 year versus 2 years	2 years	Change from baseline to 2 years (%)	*P* value	Baseline	Baseline versus 1 year	1 year	1 year versus 2 years	2 years	Change from baseline to 2 years (%)	*P* value	20-mg versus 5-mg
Age (years)	59±7							60±6							NS
Sex (male) (%)	7 (39)							6 (33)							NS
Smoking (%)	1 (6)							2 (11)							NS
Diabetes (%)	3 (17)							2 (11)							NS
Hypertension (%)	6 (33)							6 (33)							NS
Prior stain use (%)	7 (39)							7 (39)							NS
SBP (mmHg)	126±14	NS	127±12	NS	125±12	−1	NS	126±11	NS	124±11	NS	126±9	0	NS	NS
LDL-C (mm/dl)	200±47	<0.001	107±34	NS	106±36	−47	<0.001	195±35	<0.001	129±32	NS	130±33	−33	<0.001	<0.001
TG (mg/dl)	162±50	<0.001	113±37	NS	113±35	−26	<0.001	160±85	NS	141±85	NS	125±59	−22	<0.01	NS
HDL-C (mg/dl)	62±15	NS	64±16	NS	65±15	+5	NS	63±14	NS	64±11	NS	65±12	+3	NS	NS
hsCRP (mg/l)	0.71	<0.001	0.38	NS	0.34	−52	<0.001	0.60	<0.02	0.38	NS	0.42	−30	<0.05	NS

P value compared with the baseline. Data are presented as mean ± SD or number (%) of patients, except for hsCRP that is presented as the median value. Diabetes was defined as fasting plasma glucose level of ≥ 126 mg/dl or treated with insulin or hypoglycemic drugs. Hypertension was defined as blood pressures of ≥ 140/90 mmHg or treated with medication. HDL-C, HDL-cholesterol; hsCRP, high-sensitivity C-reactive protein; LDL-C, LDL-cholesterol; SBP, systolic blood pressure; TG, triglyceride.

plaques (31 in the 20-mg group and 32 in the 5-mg group) were followed up for 2 years. At baseline, there was no difference in VWT_{max} or VWA between the two groups. Calcification was found in 12% of thoracic and 16% of abdominal plaques in the 20-mg group versus 10% of thoracic and 19% of abdominal plaques in the 5-mg group (P = NS). Only one thoracic plaque was identified as a plaque with a lipid-rich core, as we previously reported [8].

After 2 years of treatment, a significant regression of thoracic plaques was found in the 20-mg group (−15% VWA reduction, $P < 0.001$) but not in the 5-mg group (+7%) (Fig. 1). Although the 20-mg dose induced plaque regression (−14%) from baseline to 1 year of treatment, no further regression was observed after a period from 1 year to 2 years of treatment (−1%). Regarding abdominal plaques, progression was found in the 5-mg group (+10%, $P < 0.002$), but not in the 20-mg group (+2%). However, a significant progression in the 5-mg group was observed from baseline to 1 year (+8%), but not from 1 to 2 years of treatment (+2%).

From baseline to 1 year, the VWA change in thoracic plaques correlated well with the degree of LDL-C reduction ($r = 0.61$), but there was only a weak correlation in abdominal plaques ($r = 0.30$) (Table 2). After a period from 1 year to 2 years of treatment, no significant plaque changes were found in either group (Fig. 1). However, the VWA change in thoracic plaques correlated with the LDL-C level after treatment (on-treatment LDL-C level), the degree of LDL-C reduction, and the on-treatment HDL-C level (Table 2). As shown in Fig. 2, the VWA change in thoracic plaques from 1 to 2 years of treatment correlated well with the on-treatment LDL-C level (r=0.64). No such correlations were found in abdominal plaques. In the multiple linear regression analysis (Table 3), the VWA changes from baseline to 1 year in both thoracic and abdominal plaques were related to the degree of LDL-C reduction. However, from 1 to 2 years of treatment, the VWA change in thoracic plaques was found to be related only to the on-treatment LDL-C level. Examples of plaque regression or progression are shown in Fig. 3.

Discussion

Intensive LDL-C lowering with 20-mg atorvastatin induced plaque regression in thoracic aorta. Plaque regression was found from baseline to 1 year, but no further regression was found after a period from 1 year to 2 years of treatment. From baseline to 1 year, the degree of plaque regression was related to the degree of LDL-C reduction, whereas the plaque change from 1 to 2 years of treatment was closely related to the on-treatment LDL-C levels. In the abdominal aorta, even 2-year treatment with 20-mg atorvastatin could not induce plaque regression.

Using MRI, the previous study, looking at the effect of 80-mg versus 20-mg simvastatin on thoracic aortic plaques, showed that greater LDL-C reduction was associated with a larger and faster regression [7]. Simvastatin reduced LDL-C levels by −38% and VWA in thoracic plaques by −11% at 1 year, and a further regression (−5%) was found from 1 to 2 years [6]. This study showed that 20-mg atorvastatin induced marked LDL-C reduction (−47%) and VWA reduction in thoracic plaques (−14%) after 1 year of treatment. However, no further regression (−1%) was found after a period from 1 year to 2 years of treatment. Using ultrasound, the Atorvastatin versus Simvastatin on Atherosclerosis Progression Trial reported 80-mg atorvastatin to induce marked LDL-C reduction (−50%) and a regression of carotid intima-media thickness during 2 years of treatment, but most of the regression was found at 1 year [12]. Therefore,

Fig. 1

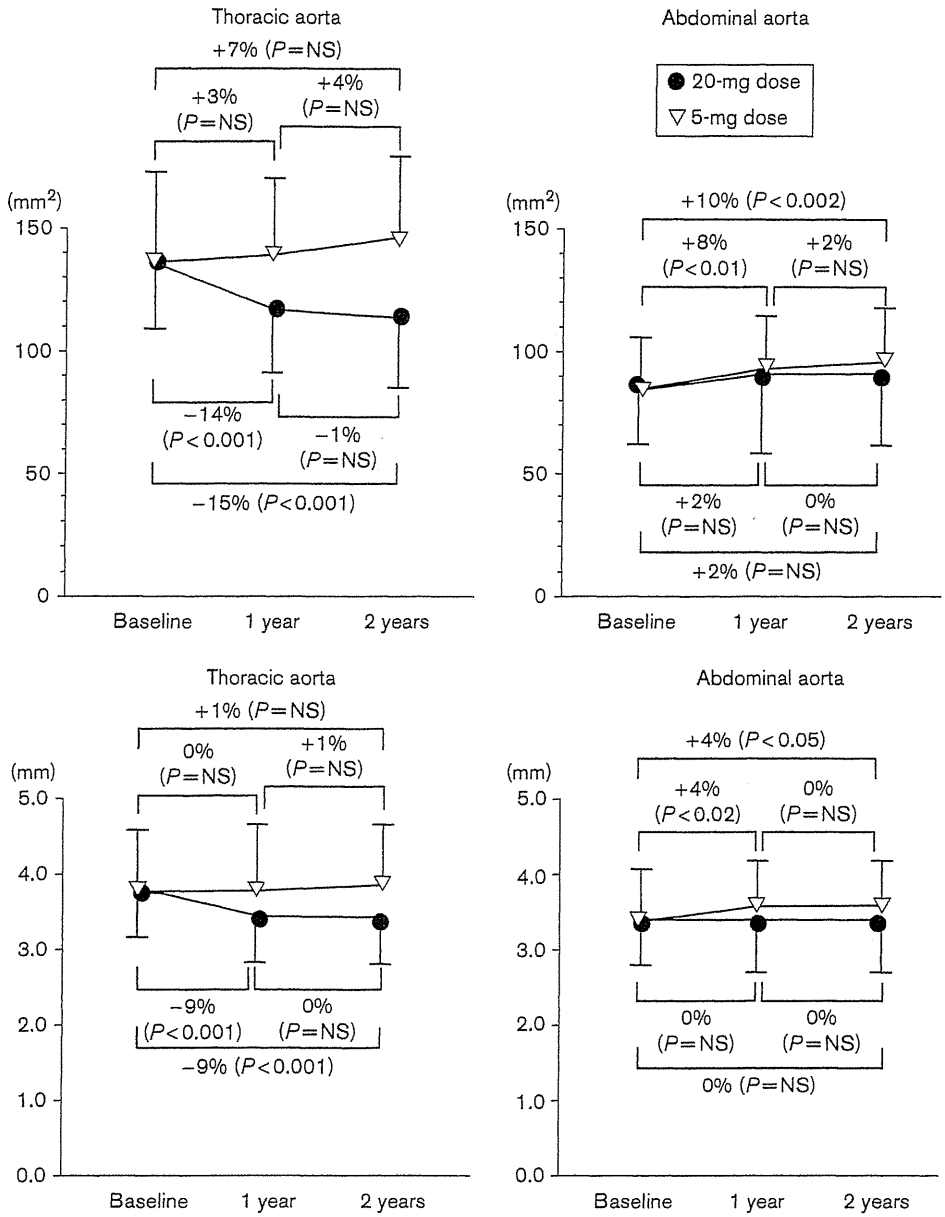

Changes in vessel wall area (VWA) and maximal vessel wall thickness after 1 and 2 years of treatment. After 2 years of treatment, a regression of thoracic plaques was found in the 20-mg group (−15% VWA reduction) but not in the 5-mg group (+7%). The 20-mg dose induced plaque regression (−14%) from baseline to 1 year, but no further regression was observed after a period from 1 to 2 years (−1%). In abdominal plaques, progression was found in the 5-mg group (+10%), but not in the 20-mg group (+2%). However, progression in the 5-mg group was found from baseline to 1 year (+8%), but not from 1 to 2 years of treatment (+2%).

greater LDL-C reduction would cause a larger and faster plaque regression, and such plaque regression would occur within 1 year of intensive LDL-C lowering therapy. Lima *et al.* [10] reported plaque regression in the thoracic aorta to be strongly associated with LDL-C reduction. This study also showed the degree of plaque regression in the thoracic aorta to closely correlate with LDL-C reduction ($r = 0.61$). The degree of LDL-C reduction appeared to be an important factor for plaque regression in the thoracic aorta.

From 1 to 2 years of treatment, the change in thoracic plaques closely correlated with the LDL-C level achieved after treatment ($r = 0.64$). This on-treatment LDL-C level was an independent factor for plaque progression in the thoracic aorta after a period from 1 to 2 years of treatment. Therefore, maintaining low LDL-C levels appeared to be an important factor for the prevention of plaque progression in the thoracic aorta. At least, maintaining LDL-C levels lesser than 110 mg/dl may be needed to prevent plaque progression in the thoracic

aorta (Fig. 2). For coronary plaques, Birgelen *et al.* [13] reported plaque area changes by intravascular ultrasound to correlate with LDL-C levels ($r = 0.41$) and an LDL-C level of less than 75 mg/dl to predict no plaque progression. Hong *et al.* [14] also reported LDL-C levels to be related to coronary plaque changes ($r = 0.47$) and an LDL-C level of less than 100 mg/dl to predict no progression. Hence, maintaining much lower LDL-C levels may therefore be needed to prevent plaque progression in the coronary arteries than in the thoracic aorta.

Table 2 Correlations between changes in vessel wall area and lipid levels: simple linear correlation coefficient

	Percent changes in VWA of thoracic aorta			
	From baseline to 1 year		From 1 to 2 years	
	r	*P* value	*r*	*P* value
On-treatment LDL-C level (mg/dl)	0.47	<0.001	0.64	<0.001
Percent change in LDL-C (%)	0.61	<0.001	0.44	<0.002
On-treatment HDL-C level (mg/dl)	−0.12	NS	−0.26	<0.05
Percent change in HDL-C (%)	0.03	NS	0.12	NS
Percent change in hsCRP (%)	0.50	<0.001	−0.20	NS
Age at baseline (years)	0.01	NS	0.14	NS
Systolic BP (mmHg)	−0.06	NS	−0.02	NS
VWA at baseline (mm^2)	−0.07	NS	−0.04	NS
	Percent changes in VWA of abdominal aorta			
On-treatment LDL-C level (mg/dl)	0.32	<0.01	0.16	NS
Percent change in LDL-C (%)	0.30	<0.01	0.17	NS
On-treatment HDL-C level (mg/dl)	−0.30	<0.01	−0.16	NS
Percent change in HDL-C (%)	−0.10	NS	−0.07	NS
Percent change in hsCRP (%)	−0.02	NS	−0.17	NS
Age at baseline (years)	0.30	<0.01	0.11	NS
Systolic BP (mmHg)	0.04	NS	−0.01	NS
VWA at baseline (mm^2)	−0.08	NS	−0.01	NS

BP, blood pressure; HDL-C, HDL-cholesterol; hsCRP, high-sensitivity C-reactive protein; LDL-C, LDL-cholesterol; SBP, systolic blood pressure; VWA, vessel wall area.

Table 3 Correlations between changes in vessel wall area and lipid levels: stepwise multiple linear regression analysis

	Percent changes in VWA of thoracic aorta			
	From baseline to 1 year		From 1 to 2 years	
	β	*P* value	β	*P* value
On-treatment LDL-C level (mg/dl)	0.29	NS	0.60	<0.002
Percent change in LDL-C (%)	0.53	<0.001	0.10	NS
On-treatment HDL-C level (mg/dl)	0.02	NS	−0.02	NS
Percent change in hsCRP (%)	0.37	<0.005	−0.21	NS
Age at baseline (years)	0.08	NS	0.18	NS
	Percent changes in VWA of abdominal aorta			
On-treatment LDL-C level (mg/dl)	0.08	NS	0.03	NS
Percent change in LDL-C (%)	0.36	<0.02	0.13	NS
On-treatment HDL-C level (mg/dl)	−0.16	NS	−0.03	NS
Percent change in hsCRP (%)	−0.08	NS	−0.11	NS
Age at baseline (years)	0.23	NS	−0.02	NS

β, regression coefficient; HDL-C, HDL-cholesterol; hsCRP, high-sensitivity C-reactive protein; LDL-C, LDL-cholesterol; VWA, vessel wall area.

Fig. 2

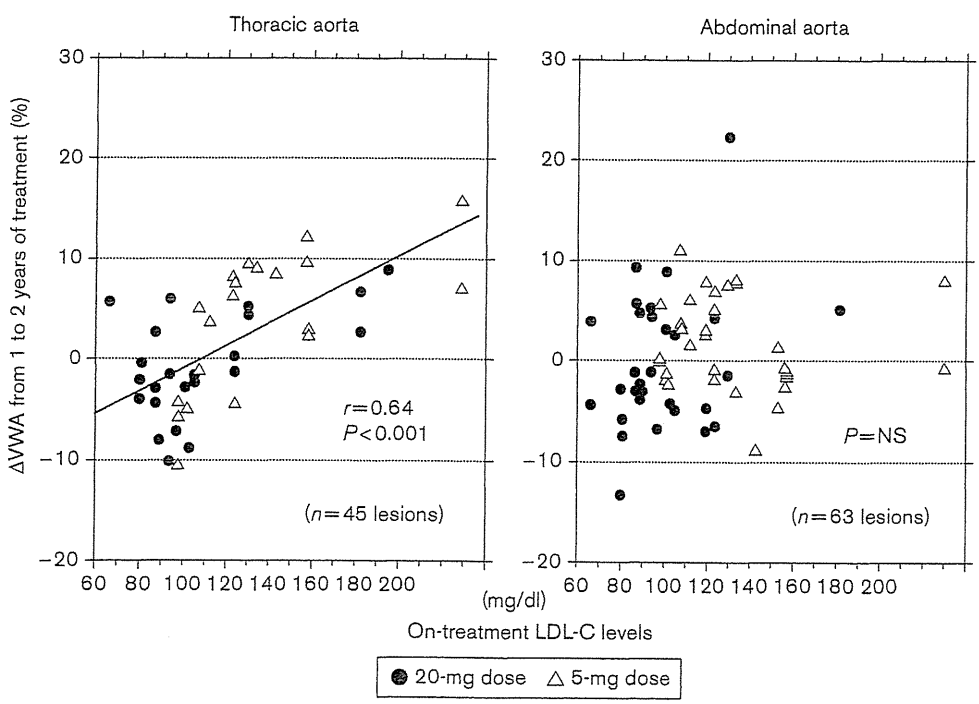

Correlations between the on-treatment LDL-C level and the percent change in VWA (ΔVWA) from 1 to 2 years of treatment. In thoracic plaques, the VWA change after a period from 1 to 2 years of treatment correlated well with the on-treatment LDL-C level ($r = 0.64$). No such correlation was found in abdominal plaques.

Fig. 3

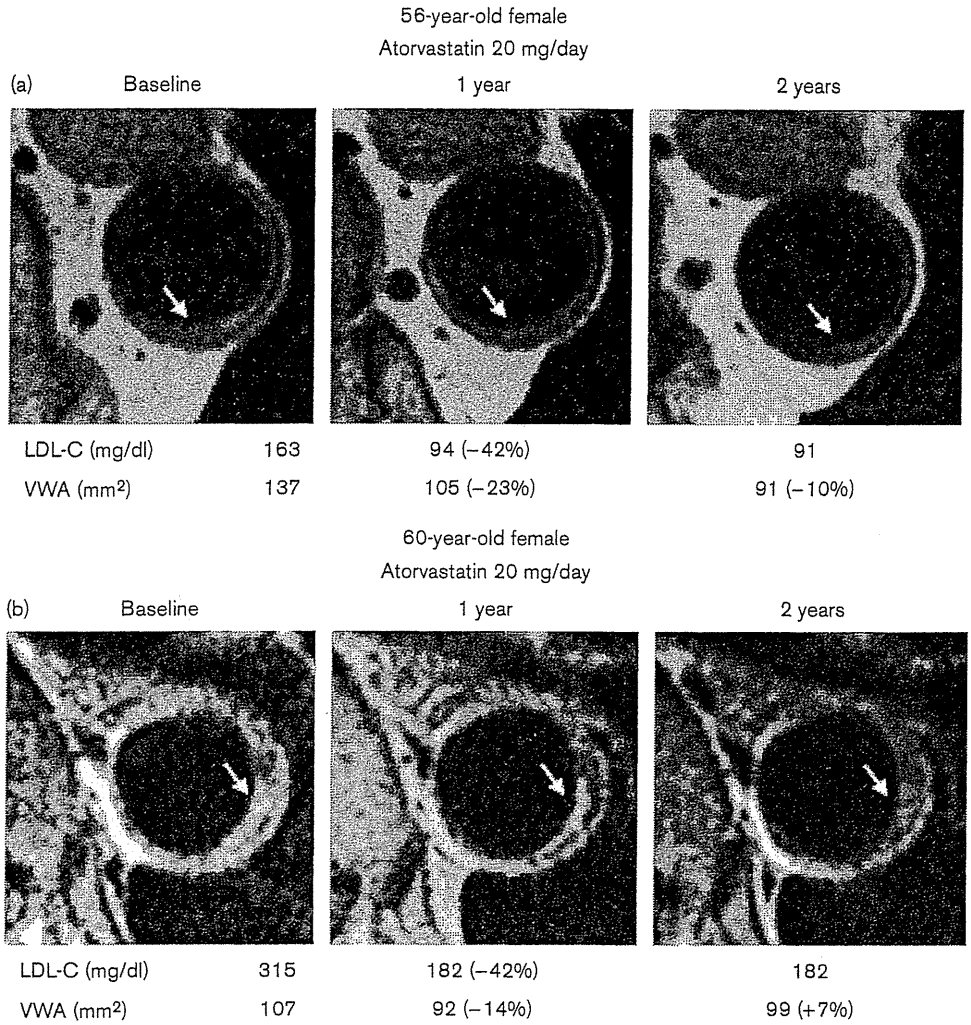

Images at baseline and after 1 and 2 years of treatment. (a) A thoracic plaque that showed a regression (−23% VWA reduction) after 1 year, by 42% LDL-C reduction with 20-mg atorvastatin. After a period from 1 to 2 years, a further regression (−10%) was found with an LDL-C level of 91 mg/dl; (b) a thoracic plaque that showed a regression (−14%) after 1 year, by 42% LDL-C reduction. However, after a period from 1 to 2 years, a progression (+7%) was observed with an LDL-C level of 182 mg/dl. Arrows indicate plaques.

Regarding abdominal plaque, even 2-year 20-mg atorvastatin could not cause regression. In rabbits fed with a cholesterol diet, the thoracic aorta showed more severe atheroma than the abdominal aorta [15]. Using ultrasonography, Tribouilloy *et al.* [16] reported an association between LDL-C levels and thoracic plaques, whereas Giral *et al.* [17] found no association between LDL-C and abdominal plaques. Using MRI, we previously reported LDL-C levels to correlate with the plaque extent in the thoracic aorta but not in the abdominal aorta [2]. Plaque formation in the thoracic aorta may thus be more closely related to LDL-C levels than in the abdominal aorta. Therefore, LDL-C lowering is more likely to be effective for plaque regression in the thoracic aorta.

Our study has several limitations. First, our study was performed on a small number of Japanese patients. The 20-mg dose was used as the higher dose of atorvastatin, because it is the maximal approved dose in Japan. The 20-mg dose is less than the dose (80 mg) in trials in Western countries [12,18]. Therefore, our results may not be applicable to other ethnic groups, but the degree of LDL-C reduction (−47%) by 20 mg in this study was similar to that with 80 mg in the Atorvastatin versus Simvastatin on Atherosclerosis Progression Trial (−50%) [12]. Second, of the 50 patients randomized, only 36 had MRI after 1 and 2 years of treatment. This may have caused some selection bias and have confounded the results. Third, all images were obtained without fat

saturation pulse, thereby causing some water–fat shift artifacts. In future studies, images should be obtained with fat saturation pulse. Finally, because TVA and VWT were measured by one observer, no interobserver variability was evaluated in our study. Therefore, the method of measurement may not be applicable to other laboratories, and further study will be needed.

In conclusion, 20-mg atorvastatin treatment induced plaque regression in the thoracic aorta. Plaque regression was, however, found from baseline to 1 year, but no further regression was found after a period from 1 to 2 years of treatment. The degree of plaque regression was related to the degree of LDL-C reduction, whereas the plaque change from 1 to 2 years of treatment was closely related to the on-treatment LDL-C levels. Maintaining low LDL-C levels thus appeared to be an important factor for preventing plaque progression. In the abdominal aorta, only the retardation of plaque progression was found, even after 2 years of 20-mg treatment. Between the thoracic and abdominal plaques, there may be some difference in the susceptibilities to LDL-C lowering and on-treatment LDL-C levels.

Acknowledgement

Our study was supported by a grant from Pfizer Co.

References

1 Fayad ZA, Nahar T, Fallon JT, Goldman M, Aguinaldo JG, Badimon JJ, *et al.* In vivo magnetic resonance evaluation of atherosclerotic plaques in the human thoracic aorta: a comparison with transesophageal echocardiography. *Circulation* 2000; **101**:2503–2509.

2 Taniguchi H, Momiyama Y, Fayad ZA, Ohmori R, Ashida K, Kihara T, *et al.* In vivo magnetic resonance evaluation of associations between aortic atherosclerosis and both risk factors and coronary artery disease in patients referred for coronary angiography. *Am Heart J* 2004; **148**:137–143.

3 Momiyama Y, Kato R, Fayad ZA, Tanaka N, Taniguchi H, Ohmori R, *et al.* A possible association between coronary plaque instability and complex plaques in abdominal aorta. *Arterioscler Thromb Vasc Biol* 2006; **26**:903–909.

4 Toussaint JF, LaMuraglia GM, Southern JF, Fuster V, Kantor HL. Magnetic resonance images lipid, fibrous, calcified, hemorrhagic, and thrombotic components of human atherosclerotic in vivo. *Circulation* 1996; **94**:932–938.

5 Helft G, Worthley SG, Fuster V, Zaman AG, Schechter C, Osende JI, *et al.* Atherosclerotic aortic component quantification by noninvasive magnetic resonance imaging: an in vivo study in rabbits. *J Am Coll Cardiol* 2001; **37**:1149–1154.

6 Corti R, Fuster V, Fayad ZA, Worthley SG, Helft G, Smith D, *et al.* Lipid lowering by simvastatin induces regression of human atherosclerotic lesions: two years' follow-up by high-resolution noninvasive magnetic resonance imaging. *Circulation* 2002; **106**:2884–2887.

7 Corti R, Fuster V, Fayad ZA, Worthley SG, Helft G, Chaplin WF, *et al.* Effects of aggressive versus conventional lipid lowering therapy by simvastatin on human atherosclerotic lesions: a prospective, randomized, double-blind trial with high-resolution magnetic resonance imaging. *J Am Coll Cardiol* 2005; **46**:106–112.

8 Yonemura A, Momiyama Y, Fayad ZA, Ayaori M, Ohmori R, Higashi K, *et al.* Effect of lipid-lowering therapy with atorvastatin on atherosclerotic aortic plaques detected by noninvasive magnetic resonance imaging. *J Am Coll Cardiol* 2005; **45**:733–742.

9 Ayaori M, Momiyama Y, Fayad ZA, Yonemura A, Ohmori R, Kihara T, *et al.* Effect of bezafibrate therapy on atherosclerotic aortic plaques detected by MRI in dyslipidemic patients with hypertriglyceridemia. *Atherosclerosis* 2008; **196**:425–433.

10 Lima JAC, Desai MY, Steen H, Warren WP, Gautam S, Lai S. Statin-induced cholesterol lowering and plaque regression after 6 month of magnetic resonance imaging-monitored therapy. *Circulation* 2004; **110**: 2336–2341.

11 Worthley SG, Helft G, Fuster V, Fayad ZA, Fallon JT, Osende JI, *et al.* High resolution ex vivo magnetic resonance imaging of in situ coronary and aortic atherosclerotic plaque in a porcine model. *Atherosclerosis* 2000; **150**:321–329.

12 Smilde TJ, van Wissen S, Wollersheim H, Trip MD, Kastelein JJ, Stalenhoef AF. Effect of aggressive versus conventional lipid lowering on atherosclerosis progression in familial hypercholesterolemia (ASAP): a prospective, randomized, double-blind trial. *Lancet* 2001; **357**:577–581.

13 Birgelen C, Hartmann M, Mintz GS, Baumgart D, Schmermund A, Erbel R. Relation between progression and regression of atherosclerotic left main coronary artery disease and serum cholesterol levels as assessed with serial long-term (12 months) follow-up intravascular ultrasound. *Circulation* 2003; **108**:2757–2762.

14 Hong MK, Lee CW, Kim YH, Park DW, Lee SW, Park CB, *et al.* Usefulness of follow-up low-density lipoprotein cholesterol level as an independent predictor of changes of coronary atherosclerotic plaque size as determined by intravascular ultrasound analysis after statin (atorvastatin or simvastatin) therapy. *Am J Cardiol* 2006; **98**:866–870.

15 Overturf M, Sybers H, Schaper J, Taegtmeyer H. Hypertension and atherosclerosis in cholesterol-fed rabbits. *Atherosclerosis* 1986; **59**:283–299.

16 Tribouilloy CM, Peltier M, Lannetta-Peltier MC, Zhu Z, Andrejak M, Lesbre JP. Relation between low-density lipoprotein cholesterol and thoracic aortic atherosclerosis. *Am J Cardiol* 1999; **84**:603–605.

17 Giral P, Pithois-Merli I, Filitti V, Levenson J, Plainfosse MC, Mainardi C, Simon AC. Prevention Cardio-vasculaire en Medecine du Travail METRA Group. Risk factors and early extracoronary atherosclerotic plaques detected by three-site ultrasound imaging in hypercholesterolemic men. *Arch Intern Med* 1991; **151**:950–956.

18 Van Wissen S, Smilde TJ, de Groot E, Hutten BA, Kastelein JJ, Stalenhoef AF. The significance of femoral intima-media thickness and plaque scoring in the Atorvastatin versus Simvastatin on Atherosclerosis Progression (ASAP) Study. *Eur J Cardiovasc Prev Rehabil* 2003; **10**:451–455.

Toxicology and Applied Pharmacology 248 (2010) 234–241

Contents lists available at ScienceDirect

Toxicology and Applied Pharmacology

journal homepage: www.elsevier.com/locate/ytaap

Hepatically-metabolized and -excreted artificial oxygen carrier, hemoglobin vesicles, can be safely used under conditions of hepatic impairment

Kazuaki Taguchi [a], Mayumi Miyasato [a], Hayato Ujihira [a], Hiroshi Watanabe [a,b], Daisuke Kadowaki [a,b], Hiromi Sakai [c], Eishun Tsuchida [c], Hirohisa Horinouchi [d], Koichi Kobayashi [d], Toru Maruyama [a,b], Masaki Otagiri [a,e,*]

[a] Department of Biopharmaceutics, Kumamoto University, 5-1 Oe-honmachi, 862-0973 Kumamoto, Japan
[b] Center for Clinical Pharmaceutical Sciences, Graduate School of Pharmaceutical Sciences, Kumamoto University, 5-1 Oe-honmachi, 862-0973 Kumamoto, Japan
[c] Research Institute for Science and Engineering, Waseda University, 3-4-1 Okubo, Shinjuku, 169-8555 Tokyo, Japan
[d] Department of Surgery, School of Medicine, Keio University, 35 Shinano Shinjyuku, 160-8582 Tokyo, Japan
[e] Faculty of Pharmaceutical Sciences, Sojo University, 4-22-1 Ikeda, 860-0082 Kumamoto, Japan

ARTICLE INFO

Article history:
Received 16 June 2010
Revised 31 July 2010
Accepted 6 August 2010
Available online 13 August 2010

Keywords:
Hemoglobin vesicle
Artificial oxygen carrier
Chronic cirrhosis
Safety and toxicology evaluations

ABSTRACT

The hemoglobin vesicle (HbV) is an artificial oxygen carrier in which a concentrated Hb solution is encapsulated in lipid vesicles. Our previous studies demonstrated that HbV is metabolized by the mononuclear phagocyte system, and the lipid components are excreted from the liver. It is well-known that many hepatically-metabolized and -excreted drugs show altered pharmaceutics under conditions of liver impairment, which results in adverse effects. The aim of this study was to determine whether the administration of HbV causes toxicity in rats with carbon tetrachloride induced liver cirrhosis. Changes in plasma biochemical parameters, histological staining and the pharmacokinetic distribution of HbV were evaluated after an HbV injection of the above model rats at a putative clinical dose (1400 mgHb/kg). Plasma biochemical parameters were not significantly affected, except for a transient elevation of lipase, lipid components and bilirubin, which recovered within 14 days after an HbV infusion. Negligible morphological changes were observed in the kidney, liver, spleen, lung and heart. Hemosiderin, a marker of iron accumulation in organs, was observed in the liver and spleen up to 14 days after HbV treatment, but no evidence of oxidative stress in the plasma and liver were observed. HbV is mainly distributed in the liver and spleen, and the lipid components are excreted into feces within 7 days. In conclusion, even under conditions of hepatic cirrhosis, HbV and its components exhibit the favorable metabolic and excretion profile at the putative clinical dose. These findings provide further support for the safety and effectiveness of HbV in clinical settings.

Introduction

Hemoglobin vesicles (HbV) are artificial oxygen carriers in which a concentrated hemoglobin (Hb) solution is encapsulated in a liposome, the surface of which is covered with polyethylene glycol (PEG). HbV has been shown to possess several superior characteristics to red blood cell (RBC) transfusion as follows: the absence of viral contamination (Abe et al., 2001), a long-term storage period of over 2 years at room temperature (Sakai et al., 2000), a low toxicity (Abe et al., 2006; Abe et al., 2007), no cross-matching and applications for use in veterinary care. It has also been clearly shown that HbV and RBC have comparable pharmacological effects in hemorrhagic shock model rats (Sakai et al., 2004c; Sakai et al., 2009). Based on these facts, HbV appears to have potential use as an alternative treatment of RBCs in cases of patients with massive blood loss. Since HbV functions as a substitute for RBC, an infused dose of HbV would be in excess of hundreds of times higher than that of other commercially available liposomal preparations such as AmBisome® or Doxil®. As a result this massive amount of HbV, with its associated components, including Hb, lipids and iron derived from Hb, could result in undesirable consequences in the systemic circulation and organs during its metabolism and disposition. Such an extraordinary appearance of HbV components could result in the accumulation of components in blood or organs, and could cause a variety of adverse effects as follows; (i) high levels of lipid components in the bloodstream,

Abbreviations: HbV, hemoglobin vesicle; Hb, hemoglobin; PEG, polyethylene glycol; RBC, red blood cell; MPS, mononuclear phagocyte system; CCl_4, carbon tetrachloride; rHSA, recombinant human serum albumin; WBC, white blood cell; Hct, hematocrit; AST, aspartate aminotransferase; ALT, alanine aminotransferase; γ-GTP, γ-glutamyl-transferase; T-bilirubin, total bilirubin; ALP, alkaline phosphatase; BUN, urea nitrogen; CRE, creatinine; TG, triglyceride; H&E, hematoxylin/eosin; PAO, potential antioxidant; TBARS, thiobarbituric acid reactive substances; ^{3}H-HbV, ^{3}H-labeled hemoglobin vesicle.

* Corresponding author. Department of Biopharmaceutics, Kumamoto University, 5-1 Oe-honmachi, 862-0973 Kumamoto, Japan. Fax: +81 96 362 7690.
E-mail address: otagiri@gpo.kumamoto-u.ac.jp (M. Otagiri).

0041-008X/$ – see front matter. Crown Copyright © 2010 Published by Elsevier Inc. All rights reserved.
doi:10.1016/j.taap.2010.08.006

especially cholesterol, which are risk factors for kidney disease, arterial sclerosis and hyperlipidemia (Grone and Grone, 2008), (ii) Hb induces renal toxicity by dissociation of the tetramic Hb subunits into two dimers (Parry, 1988), (iii) free iron can trigger tissue damage induced by the Fenton reaction, which is mediated by heme (iron) (Balla et al., 2005). Since HbV would be expected to be used in cases of emergency medical treatment, it must have favorable metabolic and excretion profiles in a wide variety of situations.

Previously, we and our colleagues carried out pharmacokinetic, histological and biochemical studies of normal rats receiving of bolus HbV injection. The results obtained from these studies clearly showed that HbV is captured and metabolized by the mononuclear phagocyte system (MPS) mainly in Kupffer cells, and the lipid components are excreted from the liver *via* the bile (Sakai et al., 2001; Sakai et al., 2004a; Taguchi et al., 2009b). Similar results were also observed in a rat model of hemorrhagic shock (Sakai et al., 2009; Taguchi et al., 2009a). These findings demonstrated that HbV appears to show favorable metabolic and excretion profiles not only in normal but under hemorrhagic conditions as well, and thus HbV can be classified as a hepatically-metabolized and -excreted drug.

In the case of a clinical situation, patients with hepatic chronic cirrhosis represent a candidate for the therapeutic application of HbV, because they frequently show upper gastrointestinal tract bleeding following the rupture of portosystemic collaterals, so-called variceal bleeding. It is well-known that the pharmacokinetic and pharmacological effects of many hepatically-metabolized and excreted drugs are impaired under conditions of liver impairment (Greenfield et al., 1983; Okumura et al., 2007). Since these changes have the potential to cause serious adverse effects, some drugs are contraindicated for a person with hepatic injury. Thus, if the HbV components also show toxic or accumulative properties under conditions of liver failure, HbV may also be contraindicated for a person with liver impairment or a dose adjustment may be necessary under such conditions. Thus, before proceeding to a clinical evaluation, it is necessary to determine whether HbV can be useful as an artificial oxygen carrier under conditions of chronic liver impairment.

The purpose of this study was to perform a toxicological assessment of HbV, such as plasma biochemical parameters, histological staining, oxidative stress and the tissue distribution of HbV, after a bolus intravenous administration of HbV at a putative dose (1400 mg Hb/kg) in rats with carbon tetrachloride (CCl_4) induced liver impairment.

Materials and methods

Materials. An Hb solution was purified from outdated donated blood provided by the Japanese Red Cross Society (Tokyo, Japan). Pyridoxal 5'-phosphate was purchased from Sigma Chemical Co. (St. Louis, MO). 1,2-dipalmitoyl-*sn*-glycero-3-phosphatidylcholine, cholesterol, and 1,5-bis-*O*-hexadecyl-*N*-succinyl-L-glutamate were purchased from Nippon Fine Chemical Co. Ltd. (Osaka, Japan). 1,2-distearoyl-*sn*-glycero-3-phosphatidyl-ethanolamine-*N*-PEG was purchased from NOF Corp. (Tokyo, Japan). Recombinant human serum albumin (rHSA) was donated by the Nipro Corp. (Osaka, Japan). CCl_4 was purchased from Wako Pure Chemical Industry Ltd. (Osaka, Japan). Mineral oil was purchased from Nakarai Chemicals, Ltd. (Kyoto, Japan).

Preparation of HbV. HbV samples were prepared under sterile conditions as previously reported (Sakai et al., 1997). The resulting encapsulated Hb (38 g/dl) contained 14.7 mM of pyridoxal 5'-phosphate as an allosteric effector to regulate P_{50} to 25–28 torr. The lipid bilayer was comprised of a mixture of 1,2-dipalmitoyl-*sn*-glycero-3-phosphatidylcholine, cholesterol, and 1,5-bis-*O*-hexadecyl-*N*-succinyl-L-glutamate at a molar ratio of 5/5/1, and 1,2-distearoyl-*sn*-glycero-3-phosphatidyl-ethanolamine-*N*-PEG (0.3 mol%). The average particle diameter was 250–280 nm. The HbVs were suspended in a physiological salt solution at 1000 mg Hb in 10 mL volume, and purged with N_2 prior to storage. The lipopolysaccharide content was <0.1 EU/mL.

Preparation of a rat model of chronic liver impairment induced by CCl_4. All animal experiments were undertaken in accordance with the guideline principles and procedures of Kumamoto University for the care and use of laboratory animals. All animals were maintained under conventional housing conditions, with food and water *ad libitum* in a temperature-controlled room with a 12 h dark/light cycle. The chronic liver injury rats were prepared as previously reported (Taguchi et al., 2010). In short, male Sprague–Dawley rats (48–51 g body weight; 3 weeks old; Kyudou Co. Kumamoto, Japan) were intraperitoneally injected with CCl_4 in mineral oil at a dose of 400 mg/kg (a volume of 0.45 mL/kg, CCl_4: mineral oil = 1:4) three times per week for 8 weeks.

Assessment of a rat model of chronic liver injury induced by CCl_4. One day after the last injection of CCl_4, the CCl_4 treated rats were anesthetized with ether. The blood samples were collected from the inferior vena cava. The ammonium concentration in blood was immediately determined by the indophenol reaction using an Ammonia-Test-Wako kit (Wako Pure Chemical Industries, Osaka, Japan). An aliquot of blood was collected for measurements of the numbers of RBC, white blood cells (WBC), platelet numbers and hematocrit (Hct). The remaining blood was centrifuged (3000 g, 10 min) to obtain plasma for the analysis of aspartate aminotransferase (AST), alanine aminotransferase (ALT), γ-glutamyltransferase (γ-GTP) and total bilirubin (T-bilirubin). All blood and plasma parameters were determined by a commercial clinical testing laboratory (SRL, Tokyo, Japan). The hepatic histopathological changes between control and CCl_4 treated rats were observed by hematoxylin/eosin (H&E) stain.

Injection of an HbV suspension. One day after the last injection of CCl_4, the CCl_4 treated rats were anesthetized with ether. Subsequently, polyethylene catheters (PE 50 tubing, outer diameter equal to 0.965 mm, and inner diameter equal to 0.58 mm; Becton Dickinson and Co., Tokyo, Japan) containing saline and heparin were introduced into the left femoral vein for use in the HbV injection. Twenty-four CCl_4 treated rats were injected with an HbV suspension (1400 mg Hb/kg) containing 5% rHSA to adjust the colloid osmotic pressure of the suspension to approximately 20 mm Hg (Sakai et al., 1997), and six CCl_4 treated rats were injected with saline containing 5% rHSA. After injection, the polyethylene catheter was removed and the skin sutured with a stitch. At 1, 3, 7 and 14 days after the HbV injection, six CCl_4 treated rats were randomly selected for collection of blood and organs. After collecting blood, the rats were euthanized by acute bleeding from the abdominal aorta and organs (kidneys, liver, spleen, lungs and heart) obtained. The organs were then weighed and resected *en bloc* for a histropathological study. The organs were fixed in 4% paraformaldehyde overnight and embedded in paraffin.

Plasma biochemical parameters. Blood samples were immediately centrifuged (3000 g, 10 min) to obtain plasma. The plasma samples were then ultracentrifuged to remove HbV (50,000 g, 30 min), because HbV interferes with some of the laboratory tests (Sakai et al., 2003). All plasma samples were stored at −80 °C until used. All plasma samples were analyzed by a commercial clinical testing laboratory (SRL, Tokyo, Japan). The analyses performed were total protein, ALT, AST, albumin, γ-GTP, alkaline phosphatase (ALP), urea nitrogen (BUN), creatinine (CRE), lipase, triglyceride (TG), phospholipids, total cholesterol, cholesterol ester, HDL-cholesterol, total bilirubin, direct bilirubin, indirect bilirubin and iron (Fe).

Histopathological examination. The organs were sectioned into 5 μm slices. Morphological changes in each organ were confirmed by hematoxylin/eosin (H&E) staining. The presence and location of hemosiderin, including free iron released by the metabolism of heme, were confirmed by Berlin blue staining. In short, the paraffin sections were deparaffinized. The deparaffinized sections were washed and then incubated with the stain solution (2 w/v% $K_4[Fe(CN)_6]$ $3H_2O$, 1 v/v% HCl) for 20 min. After washing, the sections were incubated

with a second stain solution (5 w/v% aluminum sulfate, 0.1 w/v% nuclear fast red) for 5 min.

Evaluation of oxidative stress. A 'PAO' test kit (Nikken SEIL Co., Ltd., Shizuoka, Japan) following the manufacturer's instructions, was used to evaluate the potential antioxidant (PAO), which evaluates Cu^{++} reduction on behalf of all present antioxidants, in plasma. Thiobarbituric acid reactive substances (TBARS) to measure the level of lipid peroxidation in plasma and liver were determined by means of a TBARS Assay Kit (Cayman Chemical Company, Michigan, USA) following the manufacturer's instructions. The reduced and oxidized glutathione were measured by using a GSSH/GSH quantification kit (Dojindo Molecular Technologies, Inc., MD, USA).

Pharmacokinetic study. ^{3}H-HbV, in which the lipid component (cholesterol) was radiolabeled, was prepared as previously reported (Taguchi et al., 2009b). In a typical preparation, HbV was mixed with a [1,2-^{3}H(N)]-cholesterol solution, (PerkinElmer, Yokohama, Japan) and the solution incubated for 12 h at 37 °C. Before use in pharmacokinetic experiments, ^{3}H-HbV was mixed with 5% rHSA. When ^{3}H-HbV was incubated with serum (24 h, 37 °C), the ^{3}H failed to completely dissociate from the HbV.

Twelve CCl_4 treated rats were anesthetized with ether and received a single injection of a ^{3}H-HbV suspension (1400 mg Hb/kg). Six rats were randomly selected for a plasma concentration test in which the pharmacokinetic parameters were determined. The rats were anesthetized with ether, blood samples were collected at multiple time points after the ^{3}H-HbV injection (3 min, 10 min, 30 min, 1, 3, 6, 12, 24, 48 and 72 h) and the plasma was separated by centrifugation (3000 g, 5 min). At 168 h after the injection of ^{3}H-HbV, they were euthanized and the organs (kidneys, liver, spleen, heart and lungs) were collected. Urine and feces were collected at fixed intervals in a metabolic cage. Another group of six rats were euthanized at 24 h after an injection of ^{3}H-HbV, and the plasma and organs collected. The radioactivity was determined by liquid scintillation counting (LSC-5121, Aloka, Tokyo, Japan) as previously reported (Taguchi et al., 2009b).

Data analysis. Data are shown as the means ± SD for the indicated number of animals. Significant differences among each group were determined using the two-tail unpaired Student's t-test. Pharmacokinetic analyses after HbV administration proceeded based on a two-compartment model. Pharmacokinetic parameters were calculated by fitting using MULTI, a normal least-squares program (Yamaoka et al., 1981). A probability value of $p<0.05$ was considered to indicate statistical significance.

Results

Assessment of a rat model of chronic liver impairment induced by CCl_4

To evaluate the extent of hepatic impairment of the CCl_4 treated rats, we measured the levels of AST, ALT, γ-GTP, T-bilirubin and the concentration of ammonia in blood. As a result, the AST, ALT, γ-GTP and T-bilirubin levels in plasma and the concentration of ammonium in blood were significantly increased in the CCl_4 treated rats compared to those in normal rats ($p<0.01$) (Fig. 1). From the H&E staining data, hepatic damage was clearly observed in the CCR, but not in normal rats (Fig. 1F).

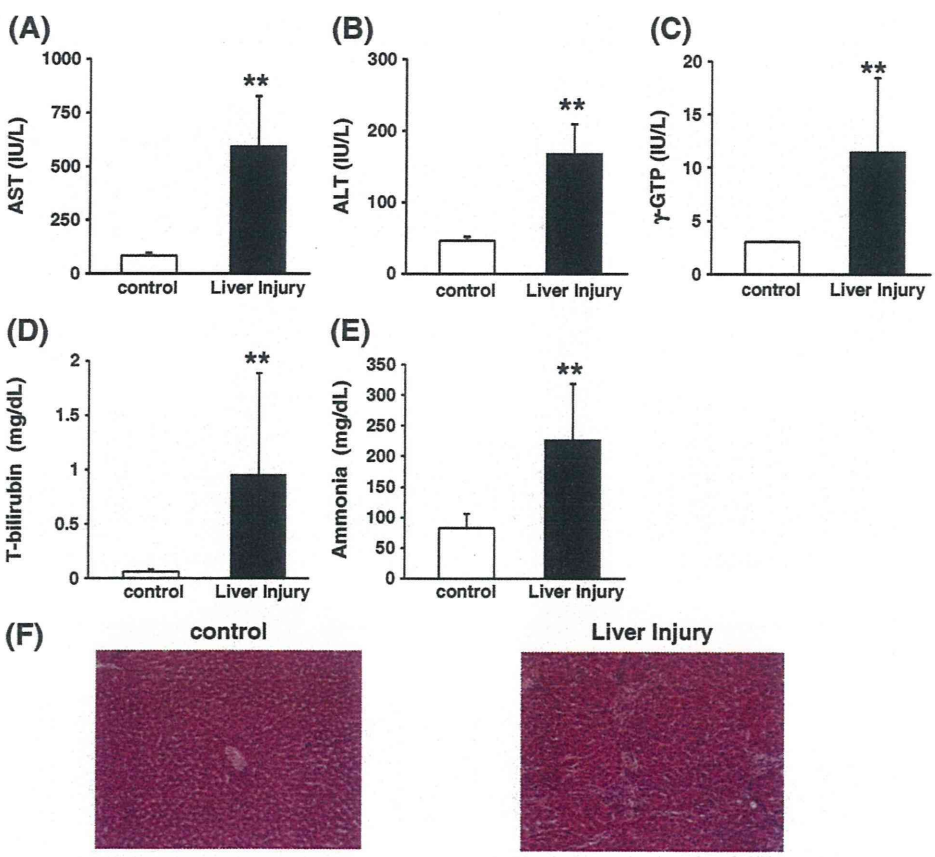

Fig. 1. Biochemical parameters (A) AST, (B) ALT, (C) γ-GTP, (D) T-bilirubin in plasma and (E) ammonia in blood in control rats (opened column) and a rat model of chronic liver injury induced by CCl_4 (closed column). (F) Light micrographs of livers stained with H&E: Control group (left) and CCl_4 treated (right) group (×100) stained with H&E. The SD rats (48–51 g body weight; 3 weeks old) were intraperitoneally injected with CCl_4 mixed with mineral oil at a dose of 400 mg/kg (a volume of 0.45 mL/kg, CCl_4: mineral oil = 1:4) three times a week for 8 weeks. One day after the last injection of CCl_4, plasma was collected and measured the biochemical parameters. The values are the mean ± SD. (n = 6) $^{**}p<0.01$ vs. control rats.

In addition, we measured the RBC, WBC, platelet numbers and Hct in the CCl_4 treated rats. The RBC, platelet and Hct levels were not significantly changed between control and CCl_4 treated rats (RBC, 712 ± 53 and $767 \pm 55 \times 10^4/\mu L$; platelet, 67.9 ± 9.0 and $63.6 \pm 17.5 \times 10^4/\mu L$; Hct, 42.6 ± 2.7 and $44.4 \pm 0.9\%$, for control and CCl_4 treated rats, respectively), while WBC in CCl_4 treated rats was increased by approximately 3-fold compared to that in normal rats (WBC, 105 ± 29 and $281 \pm 99 \times 10^2/\mu L$; $p<0.01$, for control and CCl_4 treated rats, respectively).

In addition, the changes in organ weights, which are expressed as the percentage of organ weight relative to the body weight, were measured to examine the distribution of HbV to those organs. As a result, the organ weights (kidney, liver, lung and heart) relative to body weight did not show notable changes at each day after HbV injection (data not shown). However, the spleen weight was increased by approximately 1.2-fold at 3 days after HbV injection (100 ± 14 and $118 \pm 44\%$ of baseline, $p<0.05$, for 0 day and 3 days after HbV injection, respectively), but it recovered within 14 days after the HbV injection ($100 \pm 31\%$ of baseline).

Plasma biochemical parameters representing liver. Kidney and pancreas functions

As shown in Fig. 2, the parameters reflecting liver function (AST, ALT, γ-GTP, ALP, total protein and albumin) did not show any notable changes until 7 days after HbV injection, and some (AST, ALT, γ-GTP and ALP) were decreased slightly 14 days after the HbV infusion. However, all of these values were similar with those at 14 days after a saline injection. Although, BUN and CRE, which reflect renal function, were slightly increased until 14 days after the HbV injection, these changes were still within the normal ranges. As previously reported using normal rats (Sakai et al., 2004a), the parameter reflecting pancreatic function (lipase) was temporally increased one day after HbV, but returned to the basal level within 14 days.

Plasma biochemical parameters representing the metabolism of HbV components

The levels of TG, phospholipids, total cholesterol and cholesterol ester, which are metabolites of lipid components of HbV, were significantly increased from 1 day after HbV injection, but gradually diminished to the normal level. In fact, at 14 days after the HbV injection, the concentration of the cholesterol components (total cholesterol, cholesterol ester and HDL-cholesterol) and phospholipids were not significantly different, but only the level of TG remained higher, compared with a saline injection ($p<0.01$) (Fig. 3).

T-bilirubin, direct and indirect bilirubin, which are metabolites of internal Hb decomposition, were significantly increased 1 day after the HbV injection. However, these values gradually decreased and reached the same level as those of the saline group at 14 days. Total plasma Fe, which was also released as the result of the decomposition of Hb, did not significantly changed during the period of observation (Fig. 3).

Histological examination

In a previous study, using normal rats, hemosiderin was focused in the liver and spleen after an HbV injection (Sakai et al., 2001). Therefore, we also performed Berlin blue staining to evaluate the extent of hemosiderin decomposition in liver and spleen in CCl_4 treated rats. A

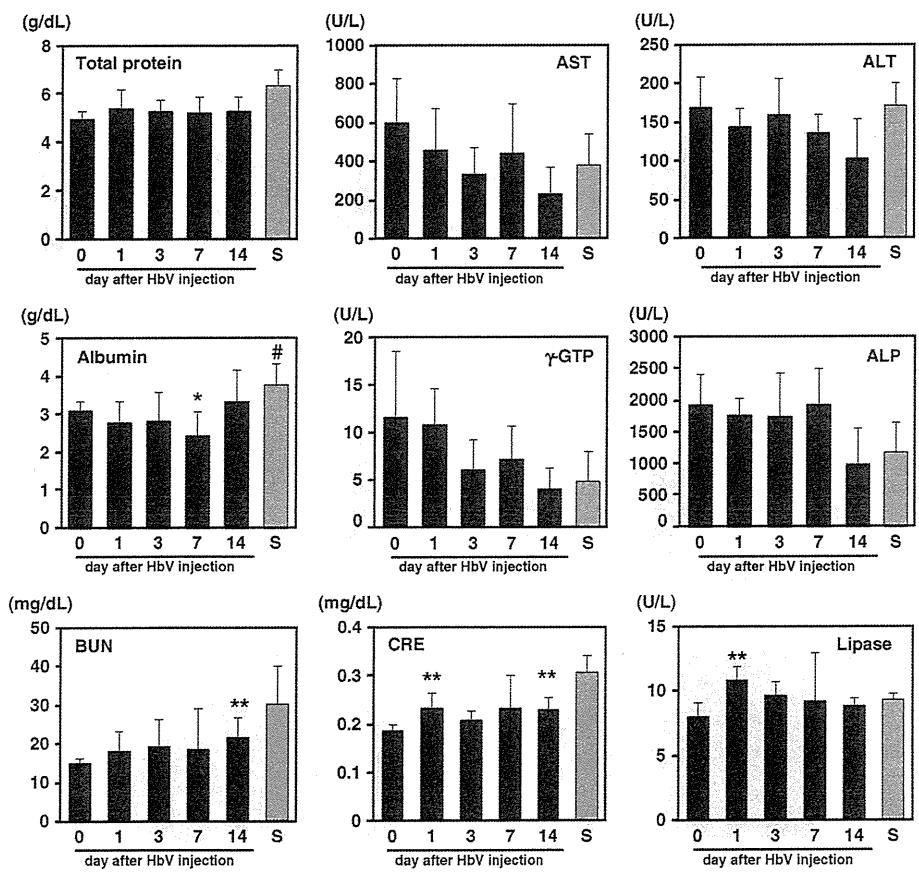

Fig. 2. Plasma biochemical parameters representing liver, kidney and pancreas function at 0, 1, 3, 7 and 14 days after HbV administration (closed column) or 14 days after a saline injection (gray column) to the rat model of chronic liver injury. The values are mean ± SD. ($n=6$) $^{*}p<0.05$, $^{**}p<0.01$ vs. before HbV infusion. $^{\#}p<0.05$ vs. 14 days after HbV infusion. S: 14 days after saline injection.

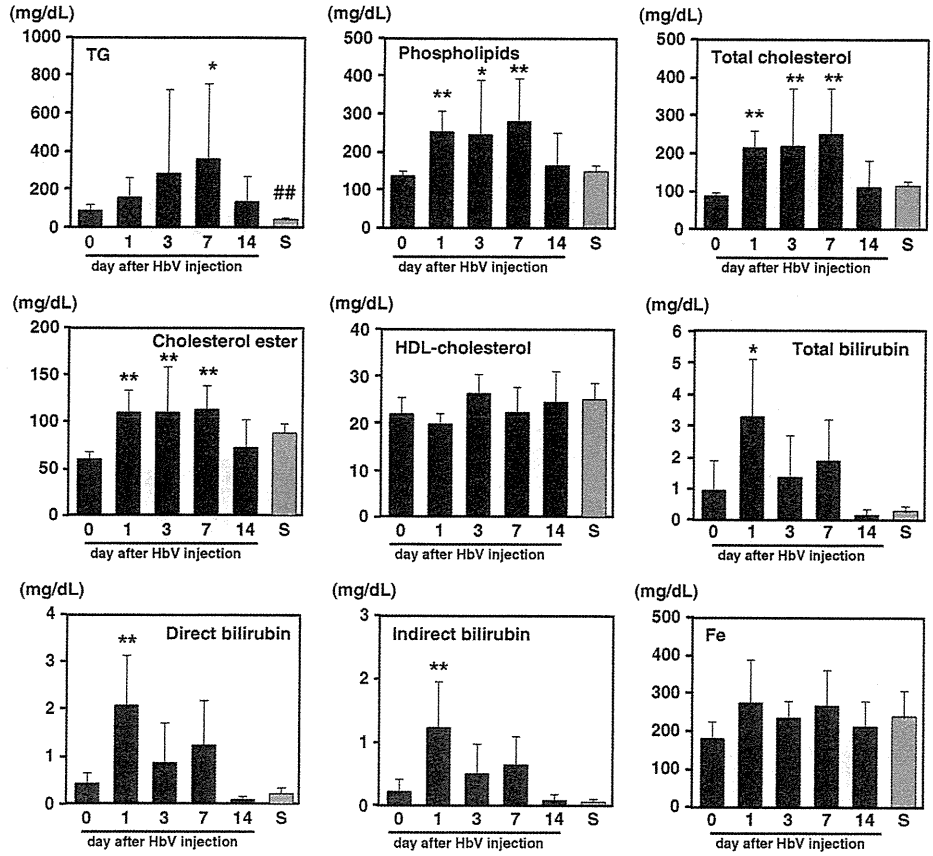

Fig. 3. Plasma biochemical parameters representing the metabolism of HbV components, such as Hb and lipid membrane, at 0, 1, 3, 7 and 14 days after the administration of HbV (closed column) or 14 days after a saline injection (gray column) to the rat model of chronic liver injury. The values are mean ± SD. (n = 6) $^{*}p<0.05$, $^{**}p<0.01$ vs. before HbV injection. $^{\#\#}p<0.01$ vs. 14 days after HbV infusion. S: 14 day after saline injection.

slight Berlin blue staining was observed in liver at days 3 and 7 (Figs. 4B and C) and a small signal was observed at 14 days after the HbV treatment (Fig. 4D). On the other hand, hemosiderin decomposition was observed in the spleen at 7 days (Fig. 4G) and at 14 days after injection of HbV (Fig. 4H). However, excessive accumulation of hemosiderin was not observed in either the liver or spleen as the result of the HbV treatment. In addition, morphological changes observed by H&E stain in kidney, liver, spleen, lung and heart were negligible after HbV injection at a dose of 1400 mg Hb/kg (data not shown).

Evaluation of oxidative stress

It has been well demonstrated that free iron enhances the production of ROS *via* the Fenton reaction, and hence, can trigger tissue damage (Balla et al., 2005). After HbV is metabolized, the heme (free iron) is released and this could induce an increase in oxidative stress. To probe this possibility further, the effect of HbV treatment on oxidative stress in plasma and liver was evaluated by measurements of TBARS and PAO. As a result, the PAO and TBARS values for plasma remained essentially unchanged as the result of HbV administration (Figs. 5A and B). In addition, the TBARS values for the liver were also determined 14 days after the HbV injection. Similar to the controls (saline treatment), a slight increase in TBARS levels in the liver was observed after the HbV infusion (0.53 ± 0.25 and 0.33 ± 0.20 μmol/L, for both the HbV and saline infusion, respectively), but the increases were not significant. To further elucidate the tissue damage by oxidative stress, the reduced and oxidized glutathione were determined. The ratio of reduced and oxidized glutathione in liver and spleen did not change during the experiments (Fig. 5C).

Pharmacokinetic study

Finally, we carried out a pharmacokinetic analysis of the lipid component of HbV in CCl_4 treated rats using ^{3}H-HbV (Fig. 6). The findings show that the approximately 10% of the HbV in plasma remained at 72 h after a bolus injection of HbV in CCl_4 treated rats. The pharmacokinetic parameters calculated using the plasma concentration curve were as follows: the half-life was 30.0 ± 4.1 h, the area under the concentration-time curve was 208 ± 51 h*% of dose/mL and plasma clearance was 0.51 ± 0.11 mL/h. Similar to normal rats, the major organs where HbV is distributed were the liver and spleen in CCl_4 treated rats (Taguchi et al., 2009b), and the maximum hepatic and splenic distributions of ^{3}H-HbVs in CCl_4 treated rats were observed at 24 h after HbV injection (25.6 ± 9.2, 14.7 ± 3.5% of the injected dose, for the liver and spleen, respectively). The majority of the ^{3}H activity in CCl_4 treated rats was excreted into feces, as previously reported for normal rats (Taguchi et al., 2009b). These data indicate that the excretion pathway of lipid components derived from HbV was essentially the same for normal and CCl_4 treated rats. The findings also confirmed that the ^{3}H radioactivity had nearly completely disappeared from the plasma and each organ 168 h after the HbV injection, and simultaneously nearly 100% of ^{3}H radioactivity had been excreted.

Discussion

As described in the introduction, HbV is one of the hepatically-metabolized and -excreted drugs. In order to avoid unpredicted or unexpected adverse effects, some of these drugs are contraindicated for a subject with hepatic impairment due to the accumulation of the drug

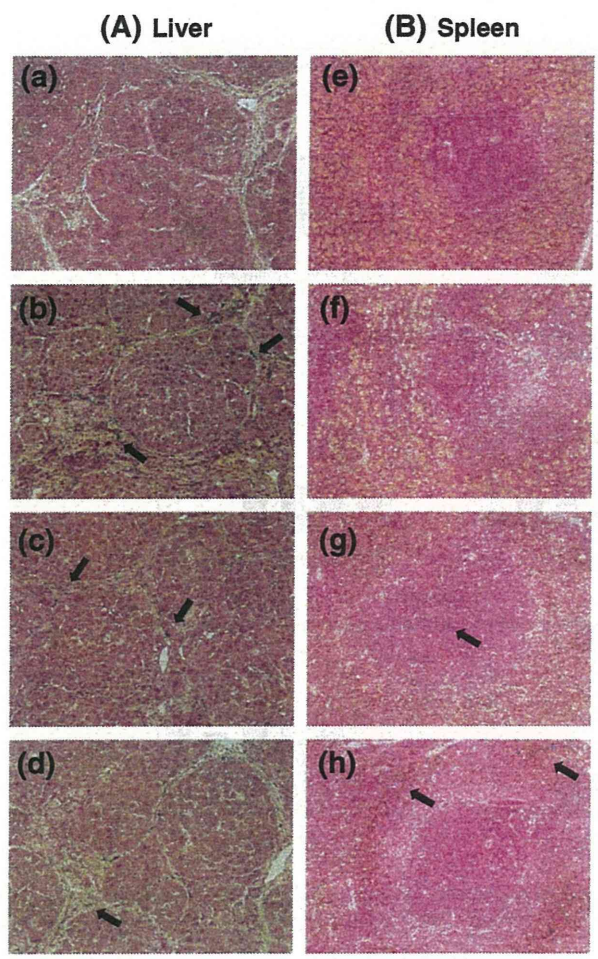

Fig. 4. Hemosiderin in liver (A) and spleen (B) in CCl_4 treated rat at 1 (a, e), 3 (b, f), 7 (c, g) and 14 (d, h) days after HbV injection stained with Berlin blue (×100). Berlin blue staining was performed to determine if hemosiderin was present. Slight hemosiderin deposition was observed in the liver at 3, 7 14 days after injection of HbV (arrow), and was also observed in the spleen at 7 and 14 days after injection of HbV (arrow).

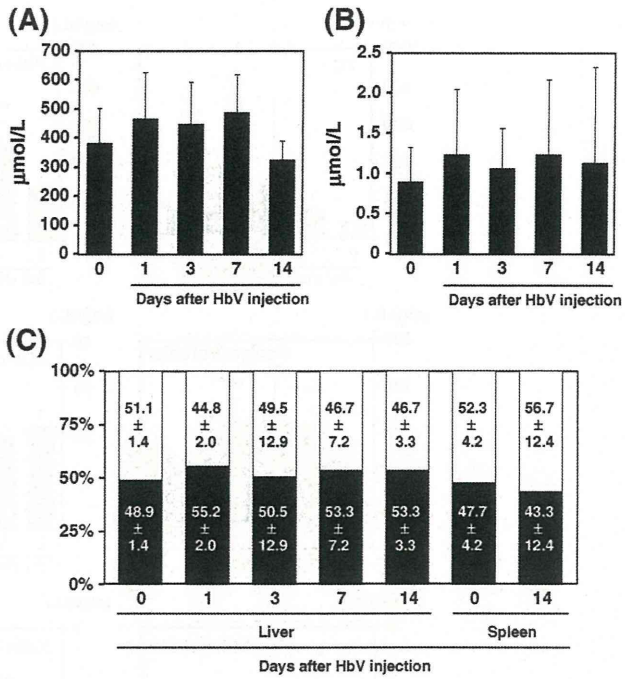

Fig. 5. Changes in the oxidative stress markers at 0, 1, 3, 7 and 14 days after HbV injection. The oxidative stress was determined by (A) potential antioxidants in plasma (PAO), (B) thiobarbituric acid reactive substances (TBARS) in plasma and (C) reduced (white) and oxidized (black) glutathione in liver and spleen. The values are the mean ± SD. (n = 6), $^{*}p<0.05$, $^{**}p<0.01$ vs. before HbV injection (0 day).

in the body. In clinical situations, a massive dose of HbV would be administered to patients, with not only hemorrhagic shock, but also hepatic chronic cirrhosis. Therefore, if HbV were to be in widespread clinical use as an RBC substitute, both therapeutic effectiveness and the safety profile in chronic liver impairment would need to be verified. In this study, we conducted the toxicological evaluation of HbV and its components, including Hb, iron derived from the heme and lipids which have the potential to be toxic in the rat model of chronic liver impairment. The results clearly demonstrate that HbV can be used safely as normal rats based on following reasons.

In the past, the perfluorocarbons have been excluded as possible candidates for artificial oxygen carriers because of the induction of chronic pneumonitis. This is due to the fact that perfluorocarbons are excreted inefficiently and accumulated in the lung, a condition that persists for more than 1 year, because perfluorocarbons was expired in a gaseous form along with the respiratory air (Nose, 2004). Thus, the long-term accumulation of an artificial oxygen carrier preparation or its components in the body must be minimized. The present study clearly showed that the half-life of HbV in the rat model of liver impairment was approximately 30 h, nearly same as that in normal rats. This suggests that HbV is not likely to accumulate in the body, even under conditions of liver failure. Since the retention in circulation is one of the therapeutic evaluation of HbV, we previously predicted that the half-life of HbV at a dose of 1400 mg Hb/kg in humans appears to be 3–4 days to use allometric equation (Taguchi et al., 2009a), and this half-life indicates that it could be used as a temporary oxygen carrier until a blood transfusion is administered or until autologous blood is recovered after a massive hemorrhage. Therefore, it would be also expected that HbV would likely possess good retention characteristics in the circulation, similar to normal conditions, even in cases of hepatic impairment.

It is well-known that the Hb derived from hemolysis and cell-free Hb based oxygen carriers (HBOCs) can induce renal and heart toxicity.

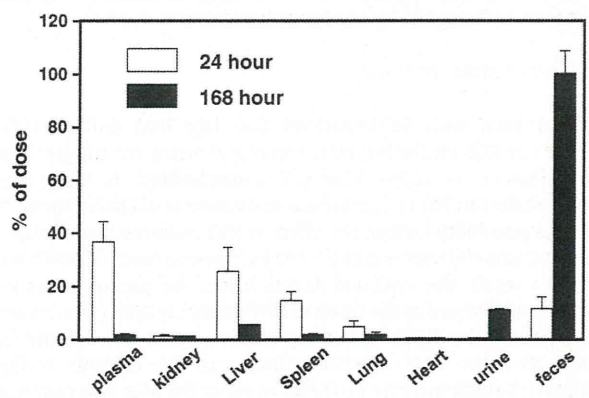

Fig. 6. The radioactivity (% of dose) in the plasma, kidney, liver, spleen, lung, heart, urine and feces at 24 (opened column) and 168 (closed column) hour after ^{3}H-HbV injection. The CCl_4 treated rats were given a single injection of ^{3}H-HbV suspension (1400 mg Hb/kg). At 24 and 168 h after the injection of ^{3}H-HbV, the rats were euthanized and organs (plasma, kidneys, liver, spleen, heart and lungs) were collected. Urine and feces were collected at fixed intervals in a metabolic cage. The values are the mean ± SD. (n = 6).

In fact, hemolysis causes renal toxicity by dissociation of tetramic Hb subunits into two dimmers, extravasaion, and precipitation in tubules (Parry, 1988). On the other hand, some of cell-free HBOCs had been excluded from proceeding to the clinical trial stage, due to the appearance of unexpected serious side effects induced by Hb. For example, diaspirin crosslinked Hb leads to the development of myocardial lesions by decreasing nitric oxide levels 24–48 h after a single topload infusion (Burhop et al., 2004), causing serious adverse effects, especially myocardial infarctions in humans (Natanson et al., 2008). Therefore, during the preclinical evaluation of HbV, the possibility of the induction of the heart and renal toxicity needs to be addressed. The findings herein indicate minimal morphological changes in heart and kidney tissue, and only negligible changes in CRE and BUN after an HbV injection at a dose of 1400 mg Hb/kg in the case of CCl_4 treated rats. This could be due to the characteristics of HbV in which its structure is maintained intact in the circulation and Hb derived from HbV was completely degraded by MPS. In fact, several results observed in this study and previous reports support these conclusions: (i) total, direct and indirect bilirubin, which were released during the metabolism of Hb, were increased from 1 day after HbV infusion, (ii) neither protein urea nor hemoglobinuria were detected in the urine in this study (data not shown), (iii) HbV is circulated in the form of stable HbV in the blood circulation until metabolized by MPS (Taguchi et al., 2009b).

Similarly, the heme (iron) is also released as a result of the metabolism of Hb, which is probably caused by the inducible form of heme oxygenase-1 in MPS in liver and spleen (Braggins et al., 1986). Generally, iron derived from heme is stored in the ferritin molecule, while overloaded iron is present as hemosiderin (Selden et al., 1980). In this study, the total Fe level in plasma was not notably changed during the period of our observations, in contrast, hemosiderin deposition was confirmed in the liver even at 14 days after HbV injection. Since hemosiderin can also release iron molecules, such released free iron could potentially induce hydroxyl radical production, and subsequently to succeed lipid peroxidation (Grady et al., 1989). However, the risk of ROS induction, as mentioned above, can be excluded in the case of HbV, because several ROS markers, such as PAO and TBARS, in the plasma did not increase during the experimental period. In addition, the TBARS level and the ratio of reduced and oxidized glutathione at 14 days after HbV injection in the liver were the same after the saline infusion. In fact, it was clearly demonstrated that the amount of iron released from hemosiderin is substantially less than that from ferritin (O'Connell and Peters, 1987). These results indicate that excess iron (heme) derived from HbV in liver impairment is likely stored as an inert form (hemosiderin) as well as that from the transfusion of RBCs and other Hb based oxygen carriers (Lenz et al., 1991; Sakai et al., 2004b).

We previously reported that the outer lipid components, especially cholesterol, were mainly eliminated to the feces *via* biliary excretion in a normal rat study (Taguchi et al., 2009b). Therefore, the possibility that these lipid components could accumulate in the body for a long period under chronic liver impairment conditions cannot be completely ignored. However, our data clearly showed that the ^{3}H-cholesterol in HbV showed a similar tissue distribution profile, mainly to the liver and spleen, as under normal conditions, and is subsequently excreted into feces within 168 h. In addition, TG, phospholipids, total cholesterol and cholesterol ester, which relate to the metabolic routes of the lipid components of HbV, were temporarily increased at 1 day after HbV infusion, but returned to normal levels within 14 days after the HbV infusion. These results indicate that the lipid components derived from HbV did not accumulate for a long period, even under hypo-metabolized and -excreted conditions.

In the present study, lipase, which reflects pancreatic function, was significantly increased on 1 day after HbV infusion. At glance, this change could be due to the damage of pancreases by HbV. However, when the pancreas is damaged, lipase levels become dramatically elevated, increasing by more than 50-fold, compared to the present data (Hofbauer et al., 1996). Thus, the small elevation of lipase level observed here can likely be attributed to the induction of pancreatic enzymes, as the result of the presence of a large amount of lipids from liposomes rather than damage caused by HbV. In fact, it has also been reported that the injection of HbV into the normal rats and liposome amphotericin B to humans also results in an increase in serum lipase activity (Stuecklin-Utsch et al., 2002; Sakai et al., 2004a).

Based on those findings, it appears likely that HbV could be safely used as an artificial oxygen carrier as an RBC substitute, even in cases of liver impairment. However, it is premature to absolutely conclude this based on the present data that was conducted under limited condition. First, in this study, we only examined the histological and biochemical parameters in a rat model of chronic liver impairment induced by CCl_4. Since the pathology of liver failure is not simple and differences in the extent of liver damage exist, such as fibrosis and injury, it will be necessary to investigate this aspect of the issue using other liver impairment animal models, for example, concanavalin A and acetaminophen induced models. Second, a previous study showed that a single high dose of HbV did not induce any change in arteriolar or venular diameters after an HbV infusion (Cabrales et al., 2005). However, Hb molecules can trigger hypertension derived by scavenging endothelium-derived nitric oxide (synthesized by NOS3) (Yu et al., 2008). In this study, changes in blood pressure, arteriolar and venular diameters were not monitored. Further study will be needed to elucidate these issues.

Recently, Zapletal et al. showed that acellular type hemoglobin-based oxygen carrier (HBOC-201) attenuated the microvascular dysfunction and improved the tissue oxygenation following the ischemic reperfusion injury in liver (Zapletal et al., 2009). Furthermore, it was reported that acellular type HBOC was useful for prehospital resuscitation with uncontrolled hemorrhage due to liver injury and hepatic cirrhosis (Ortiz et al., 2000; Arnaud et al., 2008). These results suggest that HbV and acellular type HBOC are potential candidates for alternative treatment of RBCs during liver transplantation, hepatic injury and bleeding induced by hepatic cirrhosis.

In conclusion, we demonstrate herein that HbV and its components perform favorably, in terms of metabolism and excretion, under conditions of the approximate clinical applications. These characteristics of HbV make it desirable as an alternative blood substitute, because HbV has been proposed to be used in all types of patients in multiple emergency situations including liver failure. Thus, the findings reported here provide further evidence in support of the safety and effectiveness of HbV as an oxygen carrier.

Conflict of interest statement

The authors declare that there are no conflicts of interest.

Acknowledgments

This work was supported, in part, by Health Sciences Research Grants (Health Science Research Including Drug Innovation), from the Ministry of Health, Labour and Welfare, Japan.

References

Abe, H., Ikebuchi, K., Hirayama, J., Fujihara, M., Takeoka, S., Sakai, H., Tsuchida, E., Ikeda, H., 2001. Virus inactivation in hemoglobin solution by heat treatment. Artif. Cells Blood Substit. Immobil. Biotechnol. 29, 381–388.

Abe, H., Fujihara, M., Azuma, H., Ikeda, H., Ikebuchi, K., Takeoka, S., Tsuchida, E., Harashima, H., 2006. Interaction of hemoglobin vesicles, a cellular-type artificial oxygen carrier, with human plasma: effects on coagulation, kallikrein-kinin, and complement systems. Artif. Cells Blood Substit. Immobil. Biotechnol. 34, 1–10.

Abe, H., Azuma, H., Yamaguchi, M., Fujihara, M., Ikeda, H., Sakai, H., Takeoka, S., Tsuchida, E., 2007. Effects of hemoglobin vesicles, a liposomal artificial oxygen carrier, on hematological responses, complement and anaphylactic reactions in rats. Artif. Cells Blood Substit. Immobil. Biotechnol. 35, 157–172.

Arnaud, F., Hammett, M., Philbin, N., Scultetus, A., McCarron, R., Freilich, D., 2008. Hematologic effects of recombinant factor VIIa combined with hemoglobin-based oxygen carrier-201 for prehospital resuscitation of swine with severe uncontrolled hemorrhage due to liver injury. Blood Coagul. Fibrinolysis 19, 669–677.

Balla, J., Vercellotti, G.M., Jeney, V., Yachie, A., Varga, Z., Eaton, J.W., Balla, G., 2005. Heme, heme oxygenase and ferritin in vascular endothelial cell injury. Mol. Nutr. Food Res. 49, 1030–1043.
Braggins, P.E., Trakshel, G.M., Kutty, R.K., Maines, M.D., 1986. Characterization of two heme oxygenase isoforms in rat spleen: comparison with the hematin-induced and constitutive isoforms of the liver. Biochem. Biophys. Res. Commun. 141, 528–533.
Burhop, K., Gordon, D., Estep, T., 2004. Review of hemoglobin-induced myocardial lesions. Artif. Cells Blood Substit. Immobil. Biotechnol. 32, 353–374.
Cabrales, P., Sakai, H., Tsai, A.G., Takeoka, S., Tsuchida, E., Intaglietta, M., 2005. Oxygen transport by low and normal oxygen affinity hemoglobin vesicles in extreme hemodilution. Am. J. Physiol. Heart Circ. Physiol. 288, H1885–H1892.
Grady, J.K., Chen, Y., Chasteen, N.D., Harris, D.C., 1989. Hydroxyl radical production during oxidative deposition of iron in ferritin. J. Biol. Chem. 264, 20224–20229.
Greenfield, R.A., Gerber, A.U., Craig, W.A., 1983. Pharmacokinetics of cefoperazone in patients with normal and impaired hepatic and renal function. Rev. Infect. Dis. 5 (Suppl 1), S127–S136.
Grone, E.F., Grone, H.J., 2008. Does hyperlipidemia injure the kidney? Nat. Clin. Pract. Nephrol. 4, 424–425.
Hofbauer, B., Friess, H., Weber, A., Baczako, K., Kisling, P., Schilling, M., Uhl, W., Dervenis, C., Buchler, M.W., 1996. Hyperlipaemia intensifies the course of acute oedematous and acute necrotising pancreatitis in the rat. Gut 38, 753–758.
Lenz, G., Junger, H., Schneider, M., Kothe, N., Lissner, R., Prince, A.M., 1991. Elimination of pyridoxylated polyhemoglobin after partial exchange transfusion in chimpanzees. Artif. Cells Blood Substit. Immobil. Biotechnol. 19, 699–708.
Natanson, C., Kern, S.J., Lurie, P., Banks, S.M., Wolfe, S.M., 2008. Cell-free hemoglobin-based blood substitutes and risk of myocardial infarction and death: a meta-analysis. J. Am. Med. Ass. 299, 2304–2312.
Nose, Y., 2004. Is there a role for blood substitutes in civilian medicine: a drug for emergency shock cases? Artif. Organs 28, 807–812.
O'Connell, M.J., Peters, T.J., 1987. Ferritin and haemosiderin in free radical generation, lipid peroxidation and protein damage. Chem. Phys. Lipids 45, 241–249.
Okumura, H., Katoh, M., Minami, K., Nakajima, M., Yokoi, T., 2007. Change of drug excretory pathway by CCl4-induced liver dysfunction in rat. Biochem. Pharmacol. 74, 488–495.
Ortiz, M.C., Fortepiani, L.A., de Rycker, M., Atucha, N.M., Romero, J.C., Garcia-Estan, J., 2000. Pressor and renal effects of cross-linked hemoglobin in anesthetized cirrhotic rats. J. Hepatol. 32, 32–37.
Parry, E., 1988. *Blood Substitute: Preparation, Phisiology and Medical Applications.*.
Sakai, H., Takeoka, S., Park, S.I., Kose, T., Nishide, H., Izumi, Y., Yoshizu, A., Kobayashi, K., Tsuchida, E., 1997. Surface modification of hemoglobin vesicles with poly(ethylene glycol) and effects on aggregation, viscosity, and blood flow during 90% exchange transfusion in anesthetized rats. Bioconjug. Chem. 8, 23–30.
Sakai, H., Tomiyama, K.I., Sou, K., Takeoka, S., Tsuchida, E., 2000. Poly(ethylene glycol)-conjugation and deoxygenation enable long-term preservation of hemoglobin-vesicles as oxygen carriers in a liquid state. Bioconjug. Chem. 11, 425–432.
Sakai, H., Horinouchi, H., Tomiyama, K., Ikeda, E., Takeoka, S., Kobayashi, K., Tsuchida, E., 2001. Hemoglobin-vesicles as oxygen carriers: influence on phagocytic activity and histopathological changes in reticuloendothelial system. Am. J. Pathol. 159, 1079–1088.
Sakai, H., Tomiyama, K., Masada, Y., Takeoka, S., Horinouchi, H., Kobayashi, K., Tsuchida, E., 2003. Pretreatment of serum containing hemoglobin vesicles (oxygen carriers) to prevent their interference in laboratory tests. Clin. Chem. Lab. Med. 41, 222–231.
Sakai, H., Horinouchi, H., Masada, Y., Takeoka, S., Ikeda, E., Takaori, M., Kobayashi, K., Tsuchida, E., 2004a. Metabolism of hemoglobin-vesicles (artificial oxygen carriers) and their influence on organ functions in a rat model. Biomaterials 25, 4317–4325.
Sakai, H., Masada, Y., Horinouchi, H., Ikeda, E., Sou, K., Takeoka, S., Suematsu, M., Takaori, M., Kobayashi, K., Tsuchida, E., 2004b. Physiological capacity of the reticuloendothelial system for the degradation of hemoglobin vesicles (artificial oxygen carriers) after massive intravenous doses by daily repeated infusions for 14 days. J. Pharmacol. Exp. Ther. 311, 874–884.
Sakai, H., Masada, Y., Horinouchi, H., Yamamoto, M., Ikeda, E., Takeoka, S., Kobayashi, K., Tsuchida, E., 2004c. Hemoglobin-vesicles suspended in recombinant human serum albumin for resuscitation from hemorrhagic shock in anesthetized rats. Crit. Care Med. 32, 539–545.
Sakai, H., Seishi, Y., Obata, Y., Takeoka, S., Horinouichi, H., Tsuchida, E., Kobayashi, K., 2009. Fluid resuscitation with artificial oxygen carriers in hemorrhaged rats: profiles of hemoglobin-vesicle degradation and hematopoiesis for 14 days. Shock 31, 192–200.
Selden, C., Owen, M., Hopkins, J.M., Peters, T.J., 1980. Studies on the concentration and intracellular localization of iron proteins in liver biopsy specimens from patients with iron overload with special reference to their role in lysosomal disruption. Br. J. Haematol. 44, 593–603.
Stuecklin-Utsch, A., Hasan, C., Bode, U., Fleischhack, G., 2002. Pancreatic toxicity after liposomal amphotericin B. Mycoses 45, 170–173.
Taguchi, K., Maruyama, T., Iwao, Y., Sakai, H., Kobayashi, K., Horinouchi, H., Tsuchida, E., Kai, T., Otagiri, M., 2009a. Pharmacokinetics of single and repeated injection of hemoglobin-vesicles in hemorrhagic shock rat model. J. Control. Release 136, 232–239.
Taguchi, K., Urata, Y., Anraku, M., Maruyama, T., Watanabe, H., Sakai, H., Horinouchi, H., Kobayashi, K., Tsuchida, E., Kai, T., Otagiri, M., 2009b. Pharmacokinetic study of enclosed hemoglobin and outer lipid component after the administration of hemoglobin vesicles as an artificial oxygen carrier. Drug Metab. Dispos. 37, 1456–1463.
Taguchi, K., Miyasato M., Watanabe H., Sakai, H., Tsuchida, E., Horinouchi, H., Kobayashi, K., Maruyama, T., Otagiri, M., 2010. Alteration in the pharmacokinetics of hemoglobin-vesicles in a rat model of chronic liver cirrhosis is associated with Kupffer cell phagocyte activity. J. Pharm. Sci. doi:10.1002/jps.22286.
Yamaoka, K., Tanigawara, Y., Nakagawa, T., Uno, T., 1981. A pharmacokinetic analysis program (multi) for microcomputer. J. Pharmacobiodyn. 4, 879–885.
Yu, B., Raher, M.J., Volpato, G.P., Bloch, K.D., Ichinose, F., Zapol, W.M., 2008. Inhaled nitric oxide enables artificial blood transfusion without hypertension. Circulation 117, 1982–1990.
Zapletal, C., Bode, A., Lorenz, M.W., Gebhard, M.M., Golling, M., 2009. Effects of hemodilution with a hemoglobin-based oxygen carrier (HBOC-201) on ischemia/reperfusion injury in a model of partial warm liver ischemia of the rat. Microvasc. Res. 78, 386–392.

0090-9556/11/3903-484–489$20.00
DRUG METABOLISM AND DISPOSITION
Copyright © 2011 by The American Society for Pharmacology and Experimental Therapeutics
DMD 39:484–489, 2011

Vol. 39, No. 3
36913/3666427
Printed in U.S.A.

Repeated Injection of High Doses of Hemoglobin-Encapsulated Liposomes (Hemoglobin Vesicles) Induces Accelerated Blood Clearance in a Hemorrhagic Shock Rat Model

Kazuaki Taguchi, Yasunori Iwao, Hiroshi Watanabe, Daisuke Kadowaki, Hiromi Sakai, Koichi Kobayashi, Hirohisa Horinouchi, Toru Maruyama, and Masaki Otagiri

Department of Biopharmaceutics (K.T., Y.I., H.W., D.K., T.M., M.O.), Center for Clinical Pharmaceutical Sciences (H.W., D.K., T.M.), Graduate School of Pharmaceutical Sciences, Kumamoto University, Kumamoto, Japan; Faculty of Pharmaceutical Sciences, Sojo University, Kumamoto, Japan (M.O.); Research Institute for Science and Engineering, Waseda University, Tokyo, Japan (H.S.); and Department of Surgery, School of Medicine, Keio University, Tokyo, Japan (K.K., H.H.)

Received October 24, 2010; accepted December 1, 2010

ABSTRACT:

The hemoglobin vesicle (HbV) is an artificial oxygen carrier in which a concentrated hemoglobin solution is encapsulated in a liposome. To apply liposome preparations in clinics, it is important to consider the accelerated blood clearance phenomenon (ABC phenomenon), which involves a loss in the long-circulation half-life after being administered repeatedly to the same animals. The objective of this study was to determine whether the ABC phenomenon is induced by repeated injection of HbV under conditions of hemorrhagic shock. We created a rat model of hemorrhagic shock and performed a pharmacokinetic study using ^{125}I-HbV, in which the Hb inside of HbV was labeled with ^{125}I. At 4 and 7 days after resuscitation from hemorrhagic shock by nonlabeled HbV (1400 mg Hb/kg), the second dose of ^{125}I-HbV (1400 mg Hb/kg) was rapidly cleared from the circulation compared with normal rats. Of interest, IgM against HbV was produced at 4 days after the first injection of HbV, but decreased at 7 days. In addition, phagocyte activity was increased at both 4 and 7 days after the first injection of HbV. These results suggest that repeated injections of HbV at a dose of 1400 mg Hb/kg induce the ABC phenomenon under conditions of hemorrhagic shock, which is strongly related to both the production of anti-HbV IgM and enhanced phagocyte activity. We thus conclude that it might be necessary to considerer the ABC phenomenon in the dose regimen of HbV treatment in clinical settings.

Introduction

Hemoglobin-based artificial oxygen carriers (HBOCs), which include cross-linked (Chen et al., 2009), polymerized (Jahr et al., 2008), and polymer-conjugated Hb (Smani, 2008), have been developed to overcome problems associated with blood transfusion, such as cross-matching, blood-bone infections (human immunodeficiency virus and hepatitis virus), and the shortage of donated blood. Several of these HBOCs are currently in the final stages of clinical evaluation. However, Natanson et al. (2008) recently performed a meta-analysis based on data from randomized controlled trials of five different acellular-type HBOCs and concluded that acellular-type HBOCs are associated with a significantly increased risk of death and myocardial infarction. This risk would be induced by the scavenging of nitric oxide (NO) by cell-free Hb, because it was reported that a reduction in NO levels in myocardial lesions is an important factor in inducing histological damage in cases of myocardial lesions (Burhop et al., 2004).

This work was supported in part by the Ministry of Health, Labor and Welfare of Japan ([Health Sciences Research Grants].

Article, publication date, and citation information can be found at http://dmd.aspetjournals.org.

doi:10.1124/dmd.110.036913.

The hemoglobin vesicle (HbV) is an artificial oxygen carrier with a cellular structure (liposome structure) similar to that of red blood cells (RBCs): highly concentrated Hb encapsulated in a phospholipid bilayer membrane with polyethylene glycol (PEG). Because this membrane reduces interactions between Hb and NO, adverse effects, such as hypertension and histological damage in myocardial lesions, are not induced, as are found for acellular-type HBOCs (Sakai et al., 2000, 2004a). In addition, there are some distinct advantages associated with the membrane structure of HbV as follows; the oxygen affinity (P_{50}) of HbV can be easily regulated by manipulating the content of an allosteric effector such as pyridoxal 5′-phosphate (Sakai and Tsuchida, 2007), an enhanced lifetime in the blood circulation compared with other types of HBOCs (Sou et al., 2005; Taguchi et al., 2009c), guarantees long-term storage for periods of more than 2 years at room temperature (Tsuchida et al., 2009). Moreover, HbV possesses oxygen transport characteristics that are comparable to those of RBCs. In fact, the pharmacological effects of HbV have been reported to be equivalent to that of RBCs, when injected into hemorrhagic shock animals (Sakai et al., 2004b, 2009). Therefore, HbV has attracted considerable attention as a potential candidate for use as an artificial oxygen carrier and has considerable promise for use in clinical settings.

ABBREVIATIONS: HBOC, hemoglobin-based artificial oxygen carrier; NO, nitric oxide; HbV, hemoglobin vesicle; RBC, red blood cell; PEG, polyethylene glycol; ABC phenomenon, accelerated blood clearance phenomenon; SD, Sprague-Dawley; HS, hemorrhagic shock; MZ, marginal zone.

It was reported that PEGylated liposomes showed some unexpected pharmacokinetic properties, the so-called accelerated blood clearance phenomenon (ABC phenomenon), in which the long-circulation half-life is lost after liposomes are administered twice to the same animals (Laverman et al., 2001; Ishida and Kiwada, 2008). Ishida et al. (2006a) proposed a mechanism for the ABC phenomenon as follows. IgM, produced in the spleen by the first injection of PEGylated liposomes, selectively binds to the second injected PEGylated liposomes and subsequent complement activation by IgM results in accelerated clearance and enhanced hepatic uptake of the second injected dose of PEGylated liposomes. In the case of HbV, there have been several explanations for the induction of the ABC phenomenon as follows: 1) HbV has a liposome structure that contains PEG; 2) our previous study, using normal mice, showed that the ABC phenomenon was not induced, but anti-HbV IgM was produced 7 days after the injection of HbV at a dose of 1400 mg Hb/kg (Taguchi et al., 2009c); and 3) the pharmacokinetic properties of HbV are altered under the various pathological conditions (Taguchi et al., 2009a, 2010). Therefore, it is possible that the pharmacokinetics of HbV become altered by repeated administration in various pathological conditions. In a clinical setting, HbV would be used to treat a massive hemorrhage, and repeated administrations would be required. If the pharmacokinetics of HbV were altered as the result of repeated injections, then the pharmacological action of HbV would probably be influenced. Therefore, it becomes necessary to clarify the pharmacokinetics associated with the repeated injection of HbV under conditions of massive hemorrhage.

The objective of the present study was to investigate whether the ABC phenomenon is induced by repeated injection of HbV under conditions of massive hemorrhage. To accomplish this, we examined changes in the pharmacokinetics of HbV, using ^{125}I-HbV [the internal Hb of HbV was directly labeled with iodine (^{125}I)], during repeated administration using a rat model of hemorrhagic shock. In addition, we further studied the mechanism of the induction of the ABC phenomenon under our experimental conditions.

Materials and Methods

Preparation of HbV. HbV was prepared under sterile conditions as reported previously (Sakai et al., 1997). In brief, an Hb solution was purified from outdated donated blood provided by the Japanese Red Cross Society (Tokyo, Japan). The encapsulated Hb (38 g/dl) contained 14.7 mM pyridoxal 5′-phosphate (Sigma-Aldrich, St. Louis, MO) as an allosteric effector to maintain the P_{50} to 25–28 Torr. The lipid bilayer was a mixture of 1,2-dipalmitoyl-*sn*-glycero-3-phosphatidylcholine, cholesterol, and 1,5-bis-*O*-hexadecyl-*N*-succinyl-L-glutamate (Nippon Fine Chemical Co. Ltd., Osaka, Japan) at a molar ratio of 5:5:1, and 1,2-distearoyl-*sn*-glycero-3-phosphatidylethanolamine-*N*-PEG (NOF Corp., Tokyo, Japan) (0.3 mol %). The size of the HbV particles was controlled at approximately 250 nm by the extrusion method used. The HbV was suspended in a physiological salt solution at [Hb] 10 g/dl, filter-sterilized (pore size 450 nm; Dismic, Toyo-Roshi, Tokyo, Japan) and bubbled with N_2 for storage. The lipopolysaccharide content was <0.1 endotoxin unit/ml.

Before all experiments, HbV was mixed with recombinant human serum albumin (Nipro Corp., Osaka, Japan) to adjust the albumin concentration of the suspension medium to 5 g/dl. Under these conditions, the colloid osmotic pressure of the suspension can be kept constant at approximately 20 mm Hg (Sakai et al., 2004b).

Preparation of Hemorrhagic Shock Model Rats. All animal experiments were performed according to the guidelines, principles, and procedures of Kumamoto University for the care and use of laboratory animals. SD rats were maintained in a temperature-controlled room with a 12-h dark/light cycle and ad libitum access to food and water. Hemorrhagic shock model rats were prepared as described in a previous report (Taguchi et al., 2009a). Hemorrhagic shock was induced by removal of 40% of the total blood volume (22.4 ml/kg). The systemic blood volume was estimated to be 56 ml/kg (Sakai et al., 2004b). After removal of the blood, the hemorrhagic shock rats were resuscitated by an infusion of isovolemic HbV (1400 mg Hb/kg, 22.4 ml/kg). After resuscitation, all rats were housed in a temperature-controlled room with a 12-h dark/light cycle with ad libitum access to food and water.

Quantitative Determination of Anti-HbV IgG and IgM. Five SD rats with hemorrhagic shock were resuscitated with isovolemic HbV (1400 mg Hb/kg, 22.4 ml/kg). Every day after injection, blood was collected from the tail vein under ether anesthesia. Plasma was collected after centrifugation (3000*g*, 5 min), and the supernatant was subsequently ultracentrifuged to remove intact HbV (50,000*g*, 30 min) (Sakai et al., 2003). The supernatant was collected as the plasma sample and was stored at −80°C until used. The IgG and IgM against HbV were detected as described in a previous report (Taguchi et al., 2009c).

Pharmacokinetic Experiments. ^{125}I-HbV was prepared as described in a previous report (Taguchi et al., 2009b). In short, ^{125}I-HbV was prepared by incubation of HbV with Na^{125}I (PerkinElmer Life and Analytical Sciences, Waltham, NA) in an Iodogen (1,3,4,6-tetrachoro-3*a*,6*a*-diphenylglycoluril) tube for 30 min at room temperature. ^{125}I-HbV was then isolated from free ^{125}I by passage through a PD-10 column (GE Healthcare, Uppsala, Sweden). More than 97% of the total iodine was bound to the internal Hb in HbV. All suspensions were mixed with recombinant human serum albumin (5 g/dl).

All rats were given water containing 5 mM sodium iodide for the duration of the experiment to avoid specific accumulation in the glandula thyreoidea. Ten SD rats were induced with hemorrhagic shock and resuscitated with HbV, and the pharmacokinetic study was performed at 4 days (n = 5) or 7 days (n = 5) after resuscitation. Normal rats (n = 5) were also used as controls. All rats were anesthetized with pentobarbital, and polyethylene catheters were inserted into the left femoral vein. After infusion of ^{125}I-HbV (1400 mg Hb/kg), blood samples were collected at multiple time points after the ^{125}I-HbV injection (3 min, 10 min, 30 min, 1 h, 6 h, 12 h, and 24 h) and the plasma was separated by centrifugation (3000*g*, 5 min). Degraded HbV and free ^{125}I were removed from plasma by centrifugation in 1% bovine serum albumin and 40% trichloroacetic acid. After collection of the final blood samples (24 h), the rats were euthanized, and the organs were excised (kidney, liver, spleen, lung, and heart), rinsed with saline, and weighed. The levels of ^{125}I in the plasma and excised organs were determined using a gamma counter (ARC-5000; Aloka, Tokyo, Japan).

Determination of Total Blood Volume. Total blood volume was determined using the Evans blue dilution technique as described previously, with minor modifications (Kuebler et al., 2004). In brief, 4 or 7 days after resuscitation, the rats received an intravenous bolus of 1 mg of Evans blue dye in 1 ml of normal saline. At 2 min after injection, blood samples (1 ml) were collected. The samples were centrifuged, and the absorbance of each sample was measured at 620 and 750 nm. The concentration of Evans blue was determined using a standard curve of Evans blue in excess plasma in correlation to the extinction at 620 nm corrected for turbidity at 750 nm. Total blood volume was calculated using the following formula: total blood volume = total plasma volume/(100% − hematocrit (percent) × (0.01) (Clavijo-Alvarez et al., 2005).

Measurements of Phagocyte Activity. Phagocyte activity was determined by the carbon clearance method, as described in a previous report (Sakai et al., 2001; Taguchi et al., 2010). Ten SD rats were induced with hemorrhagic shock and resuscitated with HbV, and carbon clearance was determined 4 days (n = 5) or 7 days (n = 5) after resuscitation. Normal healthy rats without HbV injection (n = 5) were also used as controls. In a typical experiment, rats were anesthetized with pentobarbital. Polyethylene catheters (PE-50 tubing) containing saline and heparin were then introduced into the left femoral vein for the infusion of a carbon particle solution and for blood collection. The carbon particle solution (Fount India Ink; Pelikan, Hannover, Germany) was infused at 10 ml/kg within 1 min. At 4, 10, 20, 30, 45, and 60 min later, approximately 100 μl of blood was then withdrawn, and precisely a 50-μl aliquot was diluted with 5 ml of a 0.1% sodium bicarbonate solution. The absorption was measured at 675 nm by means of a spectrophotometer (U-2900; Hitachi, Tokyo, Japan). The phagocyte index (K) was calculated using the equation $K = 1/(t_2 - t_1) \times \ln(C_1/C_2)$, where C_1 and C_2 are the concentrations (absorbance) at time t_1 and t_2 (min), respectively.

Measurement of Carbon Activity (CH50). Ten SD rats were induced with hemorrhagic shock and resuscitated with HbV, and blood samples were col-

lected at 4 or 7 days after resuscitation. The blood was centrifuged (3000*g*, 5 min) to obtain plasma for analysis. All plasma samples were stored at −80°C before analysis by a commercial clinical testing laboratory (SRL, Tokyo, Japan). The CH50 was detected by the method of Mayer (1961).

Data Analysis. Data are shown as the mean ± S.D. for the indicated number of animals. Significant differences among each group were determined using the two-tail unpaired Student's *t* test. Pharmacokinetic analyses after HbV administration proceeded on the basis of a two-compartment model. Pharmacokinetic parameters were calculated by fitting using MULTI, a normal least-squares program (Yamaoka et al., 1981). A probability value of $p < 0.05$ was considered to indicate statistical significance.

Results

Production of Anti-HbV IgG and IgM. In a previous study, it was reported that anti-liposome IgM, produced by the preinjection of PEGylated liposomes, is strongly involved in the induction of the ABC phenomenon (Ishida et al., 2006b). Therefore, we examined the issue of whether anti-HbV IgG and IgM are produced by an initial injection of HbV at a dose appropriate for clinical use (1400 mg Hb/kg) in the rat model of hemorrhagic shock. As shown in Fig. 1, the levels of anti-HbV IgG were negligibly increased after the injection of HbV. In contrast, anti-HbV IgM was elicited starting at 3 days after resuscitation by HbV. The highest value was found at 4 days and gradually decreased until 7 days after the injection of HbV. These results suggest that repeated injection of HbV might induce the ABC phenomenon, even under conditions of hemorrhagic shock. The following experiments were performed at the time points of 4 days ($HS_{4\ day}$) and 7 days ($HS_{7\ day}$) after resuscitation by HbV.

Pharmacokinetic Study. The fate of the ^{125}I-HbV administered to normal, $HS_{4\ day}$ and $HS_{7\ day}$ rats was evaluated by determining residual trichloroacetic acid-precipitable radioactivity in the plasma. Figure 2A shows the time course for the plasma concentration of ^{125}I-HbV in normal, $HS_{4\ day}$, and $HS_{7\ day}$ rats, and Table 1 lists the pharmacokinetic parameters for these groups. Plasma retention in the $HS_{4\ day}$ and $HS_{7\ day}$ rats decreased rapidly compared with that in normal rats, and the plasma clearance of ^{125}I-HbV in the $HS_{4\ day}$ and $HS_{7\ day}$ rats was 1.7- and 1.9-fold increased compared with that in normal rats (Table 1). Accompanied by a decrease in clearance, the area under the time-concentration curve was also significantly decreased by half, whereas the elimination-phase half-life of ^{125}I-HbV was also significantly deceased in the hemorrhagic shock model rats compared with normal rats. The pharmacokinetic parameters were not significantly different between the $HS_{4\ day}$ and $HS_{7\ day}$ rats.

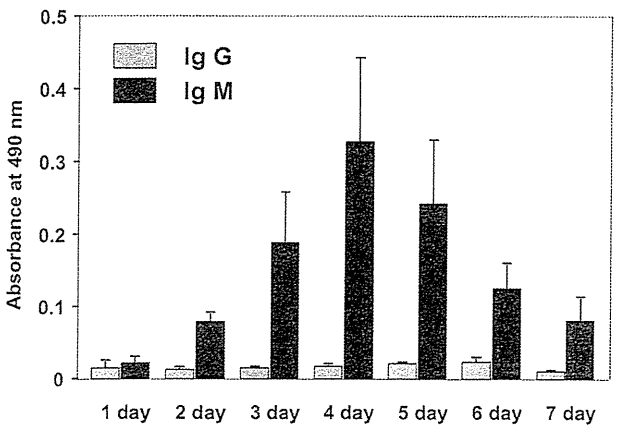

FIG. 1. The production of anti-HbV IgG and IgM after resuscitation by HbV in a rat model of hemorrhagic shock. Hemorrhagic shock was induced in SD rats with resuscitation by HbV at a dose of 1400 mg Hb/kg. After resuscitation, blood was collected from the tail vein, and plasma was obtained. Anti-HbV IgG and IgM were detected with an enzyme-linked immunosorbent assay. Each bar represents the mean ± S.D. ($n = 5$).

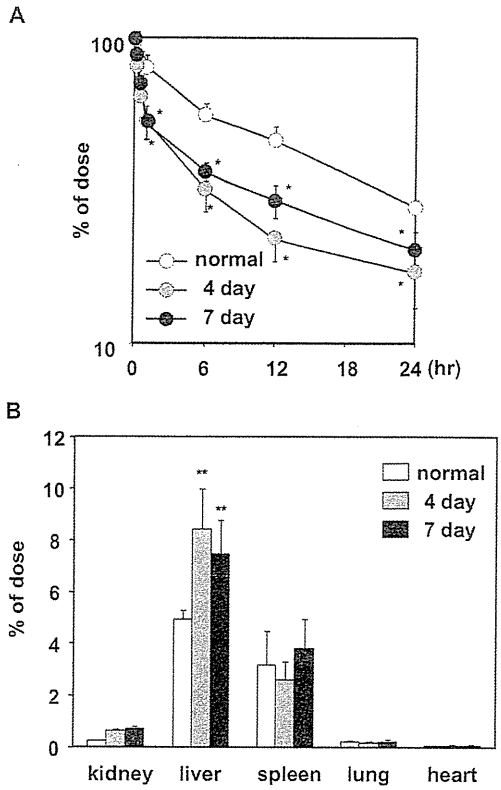

FIG. 2. A. plasma concentration curve of ^{125}I-HbV after administration to normal (○), $HS_{4\ day}$ (◌), and $HS_{7\ day}$ (●) rats at a dose of 1400 mg Hb/kg. B. tissue distributions of ^{125}I-HbV at 24 h after administration to normal (□), $HS_{4\ day}$ (▭), and $HS_{7\ day}$ (■) rats at a dose of 1400 mg Hb/kg. All rats received ^{125}I-HbV at a dose of 1400 mg Hb/kg; blood samples were collected at multiple time points (3 min, 10 min, 30 min, 1 h, 6 h, 12 h, and 24 h), and plasma samples were obtained. After collection of the final blood sample, each organ was collected at 24 h after injection. Each point represents the mean ± S.D. ($n = 5$). **, $p < 0.01$ versus normal rats.

Figure 2B shows the tissue distribution of ^{125}I-HbV (percentage of injected dose) at 24 h after ^{125}I-HbV administration. Similar to normal rats, in the $HS_{4\ day}$ and $HS_{7\ day}$ rats ^{125}I-HbV was mainly distributed in the liver and spleen. However, the amount of ^{125}I-HbV distribution in the liver was significantly increased in the $HS_{4\ day}$ and $HS_{7\ day}$ rats compared with that in normal rats, whereas that in the spleen was not significantly different among the three groups. These data indicate that the ABC phenomenon is induced in $HS_{4\ day}$ and

TABLE 1

Pharmacokinetic parameters for HbV after injections of ^{125}I-HbV in normal and hemorrhagic shock model rats

All rats received an injection of ^{125}I-HbV (1400 mg Hb/kg) containing 5% recombinant human serum albumin. At each time after the ^{125}I-HbV injection, blood was collected from the tail vein, and plasma was obtained. Each parameter was calculated by MULTI using the two-compartment model. The values are mean S.D. ($n = 5$).

	Normal	4 day	7 day
$t_{1/2\alpha}$ (h)	5.3 ± 3.9	0.53 ± 0.07*	0.47 ± 0.22*
$t_{1/2\beta}$ (h)	30.6 ± 4.0	22.3 ± 3.5*	22.0 ± 3.2*
Ke ($\times 10^3$ min^{-1})	0.70 ± 0.06	1.40 ± 0.38*	1.25 ± 0.18*
AUC (h % of dose/ml)	210.3 ± 22.9	115.9 ± 24.1*	129.4 ± 12.1*
CL (ml/h)	0.47 ± 0.04	0.90 ± 0.21*	0.78 ± 0.07*

$t_{1/2\alpha}$, the distribution-phase half-life; $t_{1/2\beta}$, the elimination-phase half-life; AUC, area under the concentration-time curve; CL, clearance.

* $p < 0.01$ versus normal.

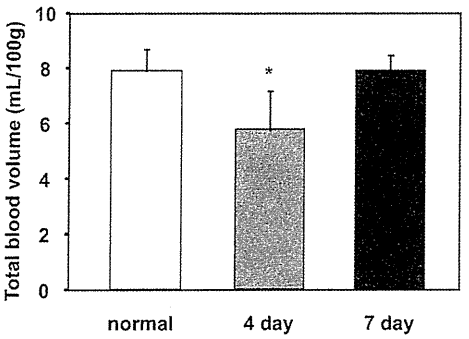

FIG. 3. Measurement of total blood volume in normal (□), $HS_{4\ day}$ (▒), and $HS_{7\ day}$ (■) rats. All rats received an intravenous bolus of 1 mg of Evans blue dye in 1 ml of NaCl. After 2 min of distribution time, blood samples (1 ml) were taken; the samples were centrifuged and the absorbance of the samples was measured at 620 and 750 nm. Total blood volume was calculated using the following formula: total blood volume = total plasma volume/(100% − hematocrit (%) × (0.01). Each bar represents the mean ± S.D. (n = 5). *, $p < 0.05$ versus normal rats.

$HS_{7\ day}$ rats, and this would be accompanied by an increased distribution in the liver.

Measurement of Total Blood Volume. It was previously observed that the retention of HbV in the circulation was decreased when the systemic blood volume decreased (Taguchi et al., 2009a). Therefore, we measured the total blood volume in normal, $HS_{4\ day}$, and $HS_{7\ day}$ rats using the Evans blue dilution technique. As shown in Fig. 3, the total blood volume in the $HS_{4\ day}$ rats was significantly changed, but this change was not remarkable compared with the massive bleeding. These data indicate that the shorter retention in the circulation in the $HS_{4\ day}$ and $HS_{7\ day}$ rats was not due to a decreased systemic blood volume and that other factors are strongly involved in this phenomenon.

Complement Activity. It is well known that the ABC phenomenon is induced by the selective binding of anti-liposome IgM to the second injected PEGylated liposomes, and subsequent complement activation by IgM results in accelerated clearance and enhanced hepatic uptake of the second injected PEGylated liposomes (Ishida and Kiwada, 2008). Therefore, we also measured the complement activity (CH50) in normal healthy, $HS_{4\ day}$, and $HS_{7\ day}$ rats.

As a result, the CH50 in $HS_{4\ day}$ and $HS_{7\ day}$ rats was significantly decreased compared with that in normal rats [38.0 ± 7.9/ml, 17.1 ± 9.4/ml ($p < 0.01$), and 30.8 ± 11.0/ml ($p < 0.05$), for normal, $HS_{4\ day}$, and $HS_{7\ day}$ rats, respectively]. However, the degree of the difference between normal healthy and $HS_{7\ day}$ rats was remarkably less than that observed between normal healthy and $HS_{4\ day}$ rats. These results suggest that the induction of the ABC phenomenon in $HS_{4\ day}$ rats is caused by an increase in complement activation, whereas that in $HS_{7\ day}$ can be mainly attributed to other mechanisms.

Phagocyte Activity. Phagocyte activity is strongly related to hepatic uptake and the induction of the ABC phenomenon. Therefore, we hypothesized that phagocyte activity, especially in Kupffer cells, would be altered after resuscitation by HbV injection. To examine the possible changes in phagocyte activity, we estimated the carbon clearance, which is an indication of phagocyte activity in Kupffer cells (Kupffer cells phagocytes were more than 90% of the injected carbon particles).

As shown in the Fig. 4, the phagocyte activity in $HS_{4\ day}$ rats was approximately 1.5 times higher than that in normal healthy rats. Of interest, compared with normal healthy rats, phagocyte activity was doubled in the $HS_{7\ day}$ rats. These data indicate that phagocyte activity is increased after resuscitation by HbV in the rat model of hemorrhagic shock, and the enhanced phagocyte activity might affect the induction of the ABC phenomenon.

Discussion

The induction of the ABC phenomenon can be described for a time frame involving two phases: the induction phase, after the first injection, during which the immune system is primed (reflected in the production of anti-liposome IgM), and the effectuation phase, after the second injection, during which PEG liposomes are rapidly cleared from the bloodstream (reflected in the enhanced uptake by Kupffer cells) (Laverman et al., 2001). In the present study, repeated injections of HbV to a hemorrhagic shock rat model at a dose of 1400 mg Hb/kg seems to induce the ABC phenomenon, and this phenomenon appears to be strongly related to changes that occur during the induction phase, in which the anti-HbV IgM was increased, and the effectuation phase, in which the phagocyte activity in Kupffer cells becomes enhanced by the initially injected HbV.

In the case of the induction phase, it is important to consider the interaction of liposomes with the marginal zone (MZ) in the spleen, which is defined as the junction of the red pulp and white pulp, and contains macrophages, dendritic cells, and B cells (MZ B cells). It was recently proposed that the induction mechanism of anti-liposome IgM involves the localization of liposomes in a certain functional splenic compartment after intravenous injection might be essential and that interaction with immune cells, B cells (but not T cells), in the spleen is critical in the development of this immune response against liposomes (Ishida et al., 2006b, 2007). In addition, it was reported that splenic MZ B cells produce large amounts of IgM within 3 to 4 days after stimulation (Martin et al., 2001). In this study, the production of anti-HbV IgM, but not that of anti-HbV IgG, started from 3 days after the first injection of HbV for resuscitation from hemorrhagic shock (Fig. 1) as well as previous studies using normal rats. Therefore, in the case of HbV injection for a hemorrhagic shock rat model, anti-HbV IgM would be produced via an interaction with splenic MZ B cells, similar to other liposome preparations.

However, it was previously reported that the production of anti-liposome IgM is suppressed with an increase in the first injected dose, and consequently the induction of the ABC phenomenon was inhibited (Wang et al., 2007). Although the dosage amount of HbV in this study was more than 100 times higher than that of other liposome preparations, anti-HbV IgM production was also induced (Fig. 1). This difference can be attributed to differences in physicochemical properties and structure, such as particle size or charge on the surface, between HbV and liposomes used in previous studies. In fact, Demoy et al. (1999) reported that particles with different surface charges and diameters showed differences in uptake by the spleen as well as

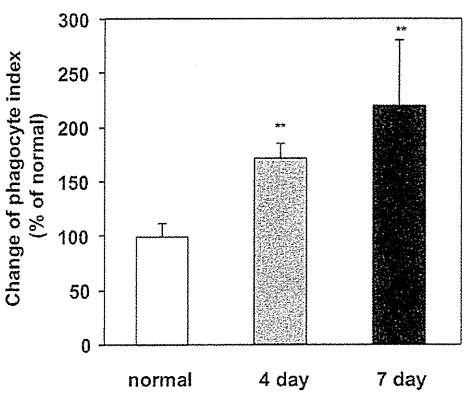

FIG. 4. The phagocyte index (K) in normal (□), $HS_{4\ day}$ (▒), and $HS_{7\ day}$ (■) rats. Carbon clearance was estimated, and K was calculated from the clearance of carbon particles. Each bar represents the mean ± S.D. (n = 5). **, $p < 0.01$ versus normal rats.

localization in the spleen compartment. The diameter and zeta potential of the HbV particles were −18.7 mV and approximately 250 nm, respectively (Tsuchida et al., 2009), whereas the liposomes used in previous reports were −1.5 mV and approximately 100 nm, respectively (Ishida et al., 2006b). In addition, senescent RBCs are finally captured and degraded by macrophages in splenic MZ cells. Because, unlike other liposomes, the structure of an HbV particle is similar to those of RBCs, it is possible that HbV would interact with MZ cells, which might play an important role in the production of anti-HbV IgM.

The effectuation phase is reflected in an enhanced uptake by the mononuclear phagocyte system, especially Kupffer cells. The carbon clearance measurements showed that systematic phagocyte activity increased by approximately 1.5- and 2-fold at 4 and 7 days, respectively, after the HbV infusion (Fig. 4). A similar phenomenon was recently reported for HbV using normal rats; systematic phagocyte activity began to increase 3 days after an HbV infusion at a dose of 2000 mg Hb/kg, and this value reached a maximum 7 days after HbV infusion (Sakai et al., 2001). From the present limited data, we cannot, with certainty, clarify the mechanism responsible for the enhancement in phagocyte activity that accompanies the administration of HbV. Previous studies reported that the composition of the lipid membrane and the size of the nanoparticles affected the phagocyte activity of mononuclear phagocyte system several days after their infusion in mice (Allen et al., 1984; Fernández-Urrusuno et al., 1996). Therefore, the physicochemical properties of HbV such as the components of the lipid membrane and particle size might also contribute to the induction of phagocyte activity.

Moreover, the possibility that the pathological conditions in our study might have had an effect on the changes in phagocyte activity cannot be excluded. It was previous reported that phagocyte activity, especially Kupffer cells, increased after hemorrhagic shock (Hunt et al., 2001). Under this condition, Kupffer cells exposed to hypoxia and reoxygenation were activated and generated oxidative stress and cytokines, which subsequently further stimulated the Kupffer cells (Rymsa et al., 1991). Moreover, primed and activated Kupffer cells are also stimulated by activated complement factors. Jaeschke et al. (1993) demonstrated that Kupffer cells were activated by complement under conditions of hepatic ischemia reperfusion. In fact, in the previous studies of HbV administration into healthy rats, the complement activation was minimal (Abe et al., 2007; Sou and Tsuchida, 2008), and the profile was significantly different from that observed in the present study. Because it is well known that ischemia reperfusion is induced even in the course of hemorrhagic shock and resuscitation, these factors might also be important for the incremental increase in phagocyte activity in this study.

To our knowledge, this is the first examination of the ABC phenomenon using a liposome preparation in conjunction with a model of a pathological condition and provides evidence for the induction of the ABC phenomenon under conditions of hemorrhagic shock. However, our model has several limitations with respect to extrapolating it for use in a human clinical setting. The present studies involved the use of a 40% bleeding model, which was indicated for an RBC transfusion in clinics. Because a massive hemorrhage frequently occurs as the result of a traffic accident or a related injury, it would be expected that the amount of bleeding would exceed 40% of total systemic blood volume. Goins et al. (1995) reported that the circulation kinetics and organ distribution vary among different hypovolemic exchange transfusions with liposome-encapsulated hemoglobin. In addition, the pathological conditions involved, such as blood flow and immunoresponses, can change with the amount of bleeding. Therefore, the induction of anti-HbV IgM and phagocyte activity might be affected by different amounts of bleeding. Similar experiments using a more severe bleeding model should be one of the subjects of future investigation. Moreover, the induction of the ABC phenomenon has been observed in mice, rats, and the rhesus monkey (Dams et al., 2000; Ishida et al., 2003). The injected time interval for the induction of the ABC phenomenon was not consistent with each animal. This implies that extrapolating the present findings obtained using a rat model to human for clinical applications is not an easy task. Therefore, it will be necessary to examine the characteristics of the ABC phenomenon among different animal models of hemorrhagic shock in determining a clinical dosage regimen for HbV.

In conclusion, the present study clearly demonstrates that repeated injections of HbV at a dose of 1400 mg Hb/kg induce the ABC phenomenon in rats under conditions of hemorrhagic shock and that this is associated with the production of anti-HbV IgM and an enhancement in phagocyte activity. These results suggest that, in a clinical situation, the repeated use of HbV in patients with a massive hemorrhage would be expected to induce the ABC phenomenon. Therefore, it may be necessary to considerer the ABC phenomenon in an administration schedule or regimen when HbV is used as a RBC substitute.

Acknowledgments

We thank Emeritus Professor Eishun Tsuchida for his support regarding our research.

Authorship Contributions

Participated in research design: Taguchi, Iwao, Watanabe, Kadowaki, and Otagiri.

Conducted experiments: Taguchi.

Contributed new reagents or analytic tools: Sakai, Kobayashi, Horinouchi, and Maruyama.

Performed data analysis: Taguchi and Kadowaki.

Wrote or contributed to the writing of the manuscript: Taguchi, Watanabe, Sakai, Maruyama, and Otagiri.

References

Abe H, Azuma H, Yamaguchi M, Fujihara M, Ikeda H, Sakai H, Takeoka S, and Tsuchida E (2007) Effects of hemoglobin vesicles, a liposomal artificial oxygen carrier, on hematological responses, complement and anaphylactic reactions in rats. *Artif Cells Blood Substit Immobil Biotechnol* **35**:157–172.

Allen TM, Murray L, MacKeigan S, and Shah M (1984) Chronic liposome administration in mice: effects on reticuloendothelial function and tissue distribution. *J Pharmacol Exp Ther* **229**:267–275.

Burhop K, Gordon D, and Estep T (2004) Review of hemoglobin-induced myocardial lesions. *Artif Cells Blood Substit Immobil Biotechnol* **32**:353–374.

Chen JY, Scerbo M, and Kramer G (2009) A review of blood substitutes: examining the history, clinical trial results, and ethics of hemoglobin-based oxygen carriers. *Clinics (Sao Paulo)* **64**:803–813.

Clavijo-Alvarez JA, Sims CA, Pinsky MR, and Puyana JC (2005) Monitoring skeletal muscle and subcutaneous tissue acid-base status and oxygenation during hemorrhagic shock and resuscitation. *Shock* **24**:270–275.

Dams ET, Laverman P, Oyen WJ, Storm G, Scherphof GL, van Der Meer JW, Corstens FH, and Boerman OC (2000) Accelerated blood clearance and altered biodistribution of repeated injections of sterically stabilized liposomes. *J Pharmacol Exp Ther* **292**:1071–1079.

Demoy M, Andreux JP, Weingarten C, Gouritin B, Guilloux V, and Couvreur P (1999) Spleen capture of nanoparticles: influence of animal species and surface characteristics. *Pharm Res* **16**:37–41.

Fernández-Urrusuno R, Fattal E, Rodrigues JM Jr, Féger J, Bedossa P, and Couvreur P (1996) Effect of polymeric nanoparticle administration on the clearance activity of the mononuclear phagocyte system in mice. *J Biomed Mater Res* **31**:401–408.

Goins B, Klipper R, Sanders J, Cliff RO, Rudolph AS, and Phillips WT (1995) Physiological responses, organ distribution, and circulation kinetics in anesthetized rats after hypovolemic exchange transfusion with technetium-99m-labeled liposome-encapsulated hemoglobin. *Shock* **4**:121–130.

Hunt JP, Hunter CT, Brownstein MR, Ku J, Roberts L, Currin RT, Lemasters JJ, and Baker CC (2001) Alteration in Kupffer cell function after mild hemorrhagic shock. *Shock* **15**:403–407.

Ishida T, Ichihara M, Wang X, and Kiwada H (2006a) Spleen plays an important role in the induction of accelerated blood clearance of PEGylated liposomes. *J Control Release* **115**:243–250.

Ishida T, Ichihara M, Wang X, Yamamoto K, Kimura J, Majima E, and Kiwada H (2006b) Injection of PEGylated liposomes in rats elicits PEG-specific IgM, which is responsible for rapid elimination of a second dose of PEGylated liposomes. *J Control Release* **112**:15–25.